American Thoracic Society

EDUCATION

2018 MTDS

AWARD WINNING ABSTRACTS

ATS

We help the world breathe®

PULMONARY • CRITICAL CARE • SLEEP

PROGRAM OVERVIEW

The American Thoracic Society (ATS) would like to congratulate the 40 Minority Trainee Development Scholarship (MTDS) awardees who are being honored at the 2018 Diversity forum for their outstanding abstracts and excellent contribution to the Society!!

The MTDS program provides an opportunity for individuals of minority status in science and medicine to travel to the ATS International Conference yearly. A unique aspect of the MTDS is that a trainee at any level (high school and beyond) who submits an abstract is eligible to be considered for this award. On average each year, the ATS receives 60+ applications and a sub-committee chaired by Dr. Yolanda Mageto, ranks applications to select the top applicants. From 2002 to 2013 this program was supported by Merck; however, in the past few years that ATS has funded this program because the Society values advancing the careers of early career professionals.

History and Results:

The MTDS program aims to address the lack of underrepresented minorities in respiratory medicine. The program was created in 2002 under the leadership of Membership and Training Committees spearheaded by Dr. Estelle Gauda in an effort to recruit the best and brightest underrepresented minorities to the field of pulmonary, critical care and sleep medicine. Each year the MTDS recipients are honored at the Diversity Forum and presented with a $1000 scholarship and a certificate of achievement.

- Over the past **17 years**, the ATS have given a total of 407 MTDS scholarships to attend the ATS International Conference.
- Out of those **17 years**, ATS has received educational support from Merck for **12 consecutive years** to provide scholarships for the MTDS.
- This is the fifth (5) consecutive year that the ATS funds the MTDS scholarships.
- Of the **407** past awardees **155 participants** are pursuing a career in Pulmonary, Critical Care and /or Sleep Medicine and **192 participants** have remained members of the ATS.
- MTDS Awardees have stated in surveys done from 2011 – 2017 that they would not have attended the ATS International Conference if it were not for the MTDS scholarship.

Criteria:

Each MTDS recipient is an author of an abstract accepted for presentation at the ATS 2018 International Conference. The awards are based on the quality of science, the contribution of the trainee to the project and the potential impact of the award on the trainee's career development. Additional award criteria includes:

- Must be a member of an underrepresented minority group as defined by the NIH (African American, Hispanic, Native American, Alaskan Native or Pacific Islander)
- Must not be a recipient of another abstract award to the 2018 ATS International Conference
- Must be a trainee (high school trough post-doctoral fellow) at a US Institution.
- Must be an author (preferably first author) of an abstract accepted for presentation at the ATS IC.

The Minority Trainee Development Scholarship (MTDS) would like to thank the American Thoracic Society for their generosity in support this program!


CONGRATULATIONS
to all Minority Trainee Development Scholarship (MTDS) AWARDEES

Extrapulmonary Expression of Surfactant Protein D and Modulation of the Gut Microbiome

Antonio Arciniegas MD, Joshua Englert MD, Rebecca Baron MD

Brigham and Women's Hospital

Background: Surfactant Protein D (SPD) is a collectin protein that plays an important role in innate immunity and host defense. SPD is produced by lung alveolar type II cells, and it has been reported to be produced by other mucosal surfaces. We unexpectedly found that SPD Knockout (KO) mice have increased survival compared to wild type (WT) mice following polymicrobial sepsis (cecal ligation and puncture, CLP) and absence of *E. Coli* in their gut microbiome, in contrast to WT mice that are colonized with *E. Coli* and become bacteremic with this organism after CLP. Furthermore, administration of recombinant SPD to SPD KO mice permitted retention of *E. Coli* in the cecum. Localization of SPD expression in the gut has been difficult to discern, and we therefore set out to test the hypothesis that SPD expression in the cecum plays an important role in regulating the microbiome and response to polymicrobial sepsis.

Methods: WT and SPD KO mice were were subjected to CLP (23g, 1 hole, 50% ligation) or sham laparotomy control. Gastrointestinal tract segments (including esophagus, stomach, duodenum, ileum, jejunum, cecum, colon), lung, pancreas, and kidney were harvested from each mouse for RNA isolation, and SPD gene expression was analyzed using quantitative PCR. Additionally, tissues were formalin fixed and paraffin embedded for future studies using in situ hybridization (RNAscope) for detection of SPD.

Results: In WT mice, as anticipated, SPD was highly expressed in the lung at baseline and after CLP. In the gastrointestinal tract, SPD message was detected only in the duodenum and stomach at baseline at substantial levels. Interestingly, 24hrs post CLP, significant induction of SPD expression was observed in the cecum, as well as in the kidney, of WT mice, while levels of expression in the duodenum were substantially reduced compared with baseline levels.

Conclusions: SPD gene expression was found in WT control mice in upper segments of the gastrointestinal tract at baseline and was induced in the cecum after sepsis. Changes in gut SPD expression may play an important role in regulation of the gut microbiome and response to sepsis. Further studies to discern SPD localization in the gut are ongoing.

Murine model of prenatal cigarette smoke exposure leads to increased cytotoxicity of lung natural killer cells in offspring

J.A. Arroyo Morales[1], H. Alikaj[2], V.R. Stolberg[2], M.R. Kady[2], J.L. Curtis[1,2], C.M. Freeman[1,2]

[1]University of Michigan Health System, Ann Arbor, MI, [2]VA Ann Arbor Healthcare System, Ann Arbor, MI

Background: Prenatal cigarette smoke (CS) exposure impairs post-natal lung development and predisposes to obstructive lung diseases via incompletely defined mechanisms. We have demonstrated increased in vitro killing of autologous lung epithelial cells by adult lung natural killer (NK) cells from both humans with COPD (relative to smokers without obstruction) and from CS-exposed mice (relative to air-exposure). We hypothesized that prenatal CS exposure programs offspring lung NK cells for enhanced post-natal cytotoxicity.

Methods: We exposed female C57BL/6 mice to either CS or air (one hour/day, five days/week) for four weeks prior to breeding. Exposures continued throughout gestation but were halted when pups were born. Without further exposure, pups were euthanized at four weeks to collect lung tissue. We reserved a portion of whole lung to characterize lung immune cell populations using flow cytometry; from the remaining lung, we isolated DX5+ NK cells, pan-dendritic cells (DCs), and CD326+ epithelial cells via immunomagnetic bead separation. We co-cultured NK cells and epithelial cells (5:1 ratio for four hours), then assayed epithelial cell apoptosis using Annexin-V plus 7-AAD staining and flow cytometry. In some experiments, lung NK cells were co-cultured overnight with lung DC before adding epithelial cells. In all experiments, epithelial cells were cultured alone as a reference.

Results: Pups exposed to prenatal CS had increased proportions of both lung NK cells and lung CD103+ DCs (as a percent of all lung leukocytes) compared to mice exposed only to air during gestation. In two independent experiments, lung NK cells from pups undergoing prenatal CS exposure were also more cytotoxic towards autologous lung epithelial cells than control pups (15.0 3.3% versus 2.6 0.9% specific cytotoxicity). There were no differences between male and female pups in either parameter. We next analyzed whether DCs from prenatal CS-exposed mice could prime naïve NK cells (from syngeneic non-exposed mice), analogous to the ability we have seen for lung DCs in human COPD to prime autolgous peripheral blood NK cells. Co-culture with DCs from air-exposed pups did not increase NK cytotoxicity. However, co-culture with lung DCs from pups that had undergone prenatal CS exposure increased cytotoxicity over NK cells alone, from 2.6 0.9% to 15.4 5.5%.

Conclusions: These data imply that CS exposure in utero increases lung NK cytotoxicity even without further CS exposure; this effect appears in part to be mediated by DC priming. NK cell dysfunction could impact immediate and long-term respiratory health.

Funding sources: Merit Review Award CX000911 from CSR&D, Department of Veterans Affairs.

Oxygen-Induced Lung Injury Is Mediated by the Lung Microbiome

S. L. Ashley[1], N. R. Falkowski[2], M. W. Sjoding[3], M. Dieterle[4], G. B. Huffnagle[5], R. P. Dickson[6]

[1]Internal Medicine, Divison of Pulmonary-Critical Care, University of Michigan, Ann Arbor, MI, United States, [2]Internal Medicine, Division of Pulmonary Critical-Care, University of Michigan, Ann Arbor, MI, United States, [3]Internal Medicine, Division of Pulmonary-Critical Care, University of Michigan, Ann Arbor, MI, United States, [4]Microbiology and Immunology, University of Michigan, Ann Arbor, MI, United States, [5]Internal Medicine - Pulmonary, University of Michigan, Ann Arbor, MI, United States, [6]Internal Medicine, Pulmonary and Critical Care Medicine, University of Michigan, Ann Arbor, MI, United States.

Rationale: Hyperoxia - elevated inspired oxygen - causes acute lung injury in animals and has been associated with increased mortality, acute respiratory distress syndrome (ARDS) and ventilator-associated pneumonia in critically ill patients. Lung-associated bacteria have variable tolerance of oxidative stress. The relationship between hyperoxia, the lung microbiome, and lung injury is unknown.

Methods: C57BL/6 mice (both conventional and Germ-Free) were exposed to room air or 95% oxygen for up to 3 days. We sampled microbiota from the lungs using a culture-independent approach (community sequencing of the 16S rRNA gene, Illumina MiSeq). We characterized lung injury in bronchoalveolar lavage fluid using a colorimetric protein assay and characterized inflammation by measuring inflammatory cytokines at various timepoints. We also studied respiratory culture isolates from human patients exposed to variable levels of oxygen via retrospective review of their medical records.

Results: Acute hyperoxia altered the lung microbiota of conventional mice, increasing relative abundance of oxygen-tolerant Staphylococcaceae ($P<0.001$) and decreasing relative abundance of oxygen-intolerant Lachnospiraceae, Clostridia, and Bacteroidia ($P<0.05$ for all). Importantly, these alterations in lung microbiota preceded the onset of peak lung injury, which was seen at day 3-post oxygen exposure. In a validation analysis of ICU patients at the University of Michigan, hyperoxia in the first 48 hours of mechanical ventilation predicted subsequent growth of Staphylococcaceae aureus from respiratory cultures ($P<0.0001$). Among genetically identical hyperoxia-exposed mice, lung bacterial diversity correlated inversely with lung concentrations of TNFα ($P=0.001$), IL-17 ($P=0.001$), and IL-4 ($P=0.01$) cytokines. Germ-free mice (genetically identical but devoid of microbiota) were protected from hyperoxia-induced lung injury as compared to conventional mice ($P<0.0001$, Figure).

Conclusions: Oxygen therapy disrupts lung microbiota in mice and humans. In mice, hyperoxia-induced lung dysbiosis is correlated strongly with lung inflammation and precedes the onset of peak lung injury. Germ-free mice are protected from oxygen-induced lung injury. These results suggest that oxygen mediates lung injury via disruption of the lung microbiome, and the lung microbiome is a previously unappreciated therapeutic target for the prevention and treatment of oxygen-induced lung injury in ARDS and ventilator-associated pneumonia.

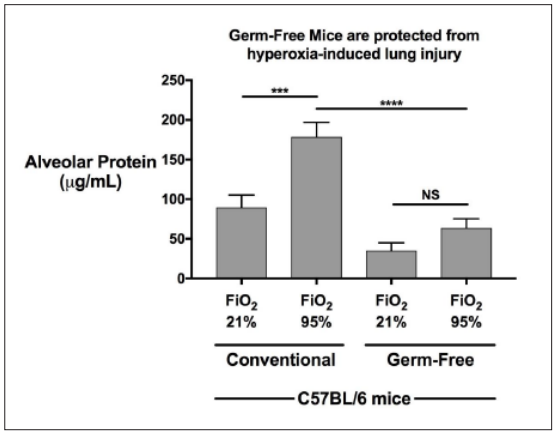

Characterizing the Role of P311 in Pulmonary Fibrosis

Fang-fang Duan, Ph.D , Gabriel M. Barron, B.S., Lucia Nieto Schuger, M.D.

University of Chicago

Rationale: Lung fibrosis can develop as a consequence of occupational or medical exposure, genetic mutations, connective tissue disease, trauma, acute lung injury leading to fibroproliferative respiratory distress syndrome, or it can develop in an idiopathic manner. Idiopathic pulmonary fibrosis (IPF), the most common form of lung fibrosis, is a progressive, irreversible and fatal scarring of lung tissue. It has been established that pro-fibrogenic transforming growth factor-β (TGF-β) is a main player in IPF. P311 is an RNA binding protein that stimulates TGF-βs 1, 2 and 3 translation through its interaction with eukaryotic translation initiation factor 3b. P311 is expressed in activated fibroblasts/myofibroblasts in both IPF and in animal bleomycin (BLM)-induced pulmonary fibrosis albeit not in the normal lung. Here, we conducted studies to determine the involvement of P311 in the lung fibrogenic process. Based on the above, we hypothesized that P311 promotes pulmonary fibrosis in part by stimulating TGF-β translation in lung fibroblasts.

Methods: Lung tissue from 6 IPF patients and 6 normal matched controls were evaluated by immunohistochemistry (IHC) for presence of P311 protein. Similarly BLM-treated mouse lungs and saline-treated controls were analyzed for P311 by immunoblot. The BLM-induced model of pulmonary fibrosis was then used to examine wild type (WT) and P311 knock-out (KO) mice for TGF-β levels/activity and standard fibrosis read-outs. In addition, primary cultures of mouse lung fibroblasts (MLFs) and human lung fibroblasts (HLFs) were transfected with P311 plasmid and assessed for standard fibrosis read-outs. Finally, we employed recombinant TGF-βs in P311 KO "rescue" experiments.

Results: IHC studies showed presence of P311 in IPF lungs but not in normal human lungs. Furthermore, P311 KOs were protected against BLM-induced pulmonary fibrosis. The KOs exhibited low levels/activity of TGF-βs 1-3 as well as decreased production of collagen I and III. In MLFs and HLFs, P311 increased TGF-βs 1-3 levels/activity; increased collagen I and collagen III levels; and promoted an activated phenotype, features commonly seen in IPF. Moreover, P311 KOs were successfully "rescued" by recombinant TGF-β 1, 2 and 3.

Conclusions:

1. P311 is highly expressed in IPF and BLM-treated lungs and absent in normal lungs.
2. P311 deficiency in mice protects against BLM-induced pulmonary fibrosis.
3. P311 expression in lung fibroblasts elicits an activated phenotype with elevated TGF-βs 1-3 levels/activity and collagens I and III, as seen in IPF.

Therapeutically, targeting P311 would reduce but not eliminate TGF-β signaling in IPF, thereby preventing the development of autoimmune complications and multiple toxicities seen with pan-TGF-βs suppression approaches

.

Mitochondrial Proteins Regulate Experimental Pulmonary Hypertension

Isabel S Bazan, MD, Jeffrey D Marshall, MD, So-Jin Kim, PhD, Peiying Shan, MD and Patty J Lee, MD

Section of Pulmonary, Critical Care & Sleep Medicine, Yale School of Medicine

Background: Pulmonary hypertension (PH) is a heterogeneous condition characterized by increased pulmonary arterial pressures and remodeling of pulmonary arteries, leading to right heart failure. The pathogenesis of PH is not well understood, but there is growing evidence that mitochondrial dysfunction may play a role. Our lab has previously shown that in an intermittent hypoxia mouse model for PH, knockout of mitochondrial uncoupling protein 2 (Ucp2) resulted in excessive PTEN-induced putative kinase 1 (PINK1)-induced mitophagy, inadequate mitochondrial biosynthesis, and increased endothelial apoptosis. It is also known that PINK1 and another mitochondrial protein, Parkin, are increased in human PH. We hypothesized that the absence of these mitochondrial proteins would protect against the development of PH in a chronic hypoxia PH mouse model.

Methods: We obtained knockout mice for PINK1 and Parkin proteins. We studied PINK1(-/-), Parkin(-/-) and wild type mice, exposed half of each group to continuous hypoxia (10% fraction of inspired oxygen) for 21 days, the other half remained at room air. All mice underwent right heart catheterizations to obtain right ventricular pressures.

Results: We found that exposure to hypoxia caused mice to have elevated right ventricular pressures consistent with PH. Neither knockout group was protected from developing PH. However, we did find that the Parkin(-/-) males had a tendency towards elevated right ventricular pressures at baseline, with little difference in pressure elevation after hypoxia compared to wild type controls.

Conclusions: Mitochondrial protein Parkin may regulate the development of experimental PH, even in the absence of hypoxia. These results also suggest that there may be gender differences in mitochondrial function, and more studies will be needed to investigate the mechanism behind this finding, the role of mitophagy and other cellular processes at play. Given the known gender differences in severity and prognosis of PH, these findings may also have a role in the pathogenesis of human PH. Moving forward, we hope to repeat this study with a larger sample size to further elucidate the gender difference, to include additional information on right heart function including right and left heart weights, and determine which cell types express PINK1 and Parkin proteins in response to chronic hypoxia.

A New Sarcoidosis Diagnostic Score

A. Bickett[1], E. E. Lower[1], R. P. Baughman[2]

[1]University of Cincinnati, Cincinnati, OH, United States, [2]Univ of Cincinnati Med Ctr, Cincinnati, OH, United States.

Background: Sarcoidosis is defined as the presence of granulomas in one or organs in the appropriate clinical setting. The purpose of this study was to develop a scoring system, the Sarcoidosis Diagnostic Score (SDS), to enhance diagnostic certainty.

Methods: Over six months, patients seen at the University of Cincinnati Sarcoidosis/Interstitial Lung Disease clinic were prospectively identified with biopsy confirmed sarcoidosis. Non-sarcoidosis patients (controls) seen at the same clinic were identified and acted as controls. For all patients, individual organ involvement was scored using World Association of Sarcoidosis and Other Granulomatous disease (WASOG) criteria with additional criteria for Lofgren's and alkaline phosphatase. Values for the various levels of organ involvement were determined using Receiver Operator Curves (ROC) developed in the initial cohort and retested in the validation cohort. Features evaluated for each organ were: biopsy, one or more highly probable symptom, one or more at least probable symptom, and one or more possible symptom. After summing the totals from each area, two components of the sarcoidosis scoring system were generated: SDS biopsy which included biopsy results and SDS clinical which did not include biopsy results.

Results: The 980 evaluable patients were dived into two cohorts: an initial 600 patients (450 biopsy confirmed sarcoidosis, 150 controls) to establish cut-off values for SDS biopsy and SDS clinical and a validation cohort of 380 patients (103 biopsy confirmed sarcoidosis patients and 277 controls). The best cutoff value for SDS biopsy was >5 and SDS clinical was >2. For SDS biopsy, the AUC was 1.000±0.0000675 (AUC±S.E.M.). The AUC for SDS clinical was 0.954±0.00785 (Figure). Similar results were seen in the validation cohort. When we combined the 980 patients, an SDS clinical score of >2 had a sensitivity of 94.2% and specificity of 88.8% and a likelihood ratio of 7.9. An SDS clinical score >3 had a sensitivity of 76.9%, specificity of 98.6%, and a likelihood ratio of 54.7.

Conclusions: his study developed two SDS scores that identified patients with sarcoidosis by compatible clinical findings with or without biopsy. This score may prove useful in diagnosing sarcoidosis.

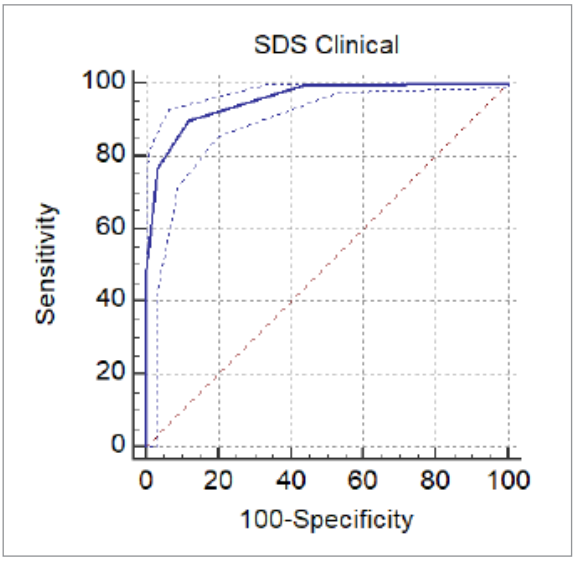

Inhibition of Equilibriative Nucleoside Transporters Protect Against *Pseudomonas aeruginosa*-Induced Acute Respiratory Distress Syndrome

Eboni Chambers, Alexis White, Alexander Vang, Zhengke Wang, Ting-Ting Mills, Gaurev Choudhary, Sharon Rounds, Alfred Ayala, Michael Blackburn, Qing Lu

Providence VA Medical Center, Department of Medicine, Alpert Medical School of Brown University, Providence, RI 02908

Acute lung injury (ALI)/acute respiratory distress syndrome (ARDS) is characterized by lung edema and inflammation. *Pseudomonas (P.) aeruginosa* infections, due to multidrug resistance, often causes ARDS particularly in patients with compromised immunity. Adenosine, a signaling nucleoside increased upon tissue injury, has been shown to protect against ALI through activation of adenosine receptors (ARs). Extracellular and intracellular adenosine concentrations are regulated by equilibriative nucleoside transporters (ENTs). Whether altering adenosine uptake can modify bacterial P. aeruginosa-induced ARDS is unknown. We hypothesize that increased extracellular adenosine by inhibiting ENT1 will protect against *P. aeruginosa*-induced ALI via activation of ARs. ENT1 pharmacological inhibitors and null mice as well as agonists and antagonists directed against adenosine receptors A2AR and A2BR were used to test this hypothesis in vivo. We found that without antibiotics treatment, *P. aeruginosa* (strain: PA103) infection induces ALI in C57BL/6 mice in a dose- and time-dependent manner. Pharmacological inhibition of ENT1 by NBTI elevates adenosine levels in bronchoalveolar lavage (BAL) fluid and significantly attenuates PA103-induced ALI, as assessed by wet-to-dry lung weight, BAL protein levels, BAL inflammatory cells, pro-inflammatory cytokines, and pulmonary function, which was evaluated by static lung compliance, tissue damping, and tissue elastance. NBTI also significantly enhances bacterial clearance in mice infected with PA103. Additionally, NBTI attenuates PA103-induced increase in lung NLRP3 and BAL IL-1β levels of mice. Consistent with ENT1 inhibitor, ENT1 null mice shows attenuated ALI and NLRP3 inflammasome activation after PA103 infection. . Agonists of A2AR and A2BR mimic NBTI blunting *P. aeruginosa*-induced ALI, whereas antagonists against A2BR diminish the protective effect of NBTI against PA103-induced ALI.. These results suggest that blocking ENT1-mediated adenosine uptake protects against *P. aeruginosa*-induced ALI via activation of A2BR and subsequent inhibition of NLRP3 inflammasome activation. Inhibition of ENT may be a novel approach to prevent and possibly treat P. aeruginosa- induced ALI.

Funding sources: This work was in part supported by NIGMS P20GM103652 to S. Rounds and Q. Lu, RO1 HL130230 to Q. Lu, PULM-019-14F to S. Rounds, and NIEHS T32 ES007272 to E. Chambers.

FBXO17 Electrode Positioning During Electrical Stimulation of the Expiratory Muscles

D. Colon Hidalgo[1], F. A. Laghi[1], A. McLachlan[2], D. Djondo[1], G. M. Pellegrino[3], G. Sferrazza Papa[3], M. J. Tobin[1], H. S. Shaikh[1]

[1]Edward Hines Jr. VAH, Loyola University Medical Center, Hines, IL, United States, [2]Liberate Medical LLC, Crestwood, KY, United States, [3]Università degli Studi di Milano, Milan, Italy.

Introduction: Electrical stimulation of the abdominal wall muscles via anteroposterior electrodes (dorsal portion latissimus dorsi-external obliques) (Fig. 1A, B) can assist breathing (Radovanovic AJRCCM 193:A7656). This electrode configuration is impractical in recumbent patients. To obviate the need for patient turning, we tested an anterolateral (anterior margin latissimus dorsi-external oblique) (Fig. 1C) and a lateral (external oblique) configuration (Fig. 1D). We hypothesized that expiratory muscle recruitment with the anterior and anterolateral configurations would not be inferior to the anteroposterior configuration.

Methods: Recordings of gastric pressure in 8 participants (4 COPD, 4 healthy), during near-maximally tolerated stimulations delivered with the three electrode configurations in random order.

Results: There was no difference in the rise in gastric pressure ($P = 0.67$) or in participants' discomfort (Wong Baker Faces Pain Rating Scale, $P = 0.14$) with each of the three configurations. Healthy subjects tolerated a higher amplitude of stimulation during anteroposterior vs. anterolateral stimulation ($P<0.01$).

Conclusions: Electrical stimulation of the expiratory muscles using anterolateral and oblique electrode configurations are practical and non-inferior to the posterolateral configuration in healthy subjects and patients with COPD.

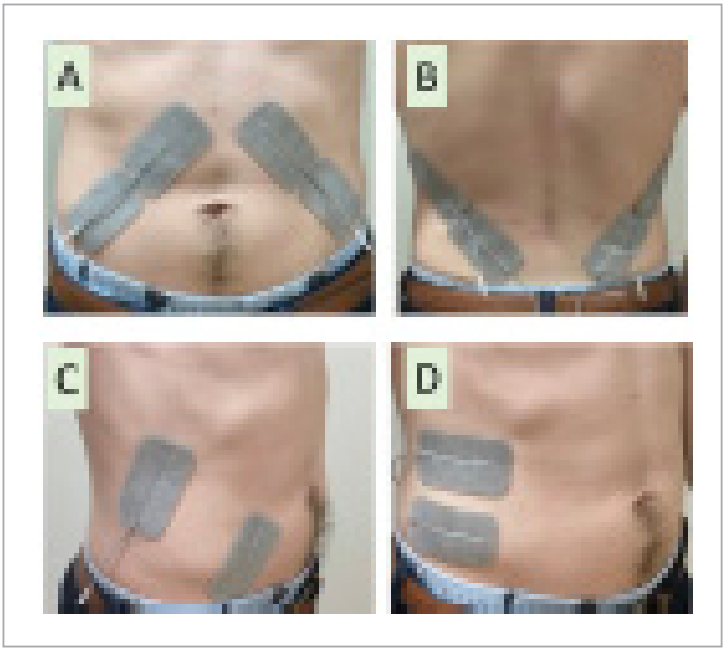

Figure 1. Electrode configurations tested. (A and B) Anteroposterior; (C) Anterolateral; (D) Lateral.

7396 –Mechanical Power in the Setting of Positive End-Expiratory Pressure (PEEP) Titrated by Esophageal Pressure

G. A. Cortes Puentes[1], F. Cipulli[2], M. Quintel[2], J. J. Marini[3], L. Gattinoni[2], R. Oeckler[1]

[1]Pulmonary and Critical Care Medicine, Mayo Clinic, Rochester, MN, United States, [2]Anesthesiology and Critical Care, University of Göttingen, Göttingen, Germany, [3]Pulmonary and Critical Care, University of Minnesota, Minneapolis, MN, United States

Rationale: Mechanical power (MP) has been postulated as the unifying variable integrating all the machine-derived factors contributing to ventilator-induced lung injury (VILI), where tidal volume, pressures, flow and respiratory rate are considered components of the inspiratory "energy load" applied to the respiratory system per unit time. We aimed to describe the behavior of both MP of the respiratory system (MPRS) and of the lung (MPL) in patients with acute respiratory distress syndrome (ARDS) while setting positive end-expiratory pressure (PEEP) during mechanical ventilation guided by esophageal pressure.

Methods: We retrospectively analyzed both the MPRS and MPL in 42 mechanically ventilated patients with ARDS in volume-controlled mode and PEEP titrated by esophageal pressure monitoring with the goal to achieve a pressure across the lung (transpulmonary pressure, PTP) of 0-10 cmH2O at the end of expiration, while maintaining an end-inspiratory PTP of <20 cmH2O. See figure 1 for equations. To estimate the energy load per unit time applied to the lung actually participating in ventilation (baby lung), MPRS and MPL were normalized by the ratio of the estimated functional residual capacity (FRC) and the compliance of the respiratory system (CRS). Variables were sub-analyzed based on ARDS severity and mortality.

Results: Among patients with moderate ARDS, non-survivors (n=9) compared to survivors (n=14) had experienced 30% more MPRS (104.9±30.1 vs. 79.7±41.7 J/min/L, mean±SD respectively, p=.012), 50% more MPL (49.8±22.3 vs. 33±19.6 J/min/L, mean±SD respectively, p=.014), and 35% greater transpulmonary driving pressure (15.8±4.5 vs. 11.7±3.9 cmH2O, mean±SD respectively, p=.012). Compared to survivors (n=8), non-surviving patients (n=3) with mild ARDS were exposed to higher PEEP values (26±4 vs. 18.1±4.3 cmH2O, mean±SD respectively, p=.0049). Mortality occurred in 17.2% with mild, 39.1% with moderate, and 37.5% of patients with severe ARDS.

Conclusions: In our study sample, mechanical ventilation with PEEP titrated by esophageal pressure monitoring resulted in unexpectedly high values of PEEP among patients with mild ARDS. Additionally, both MPRS and MPL seemed to track the higher mortality rate observed in the moderate ARDS group.

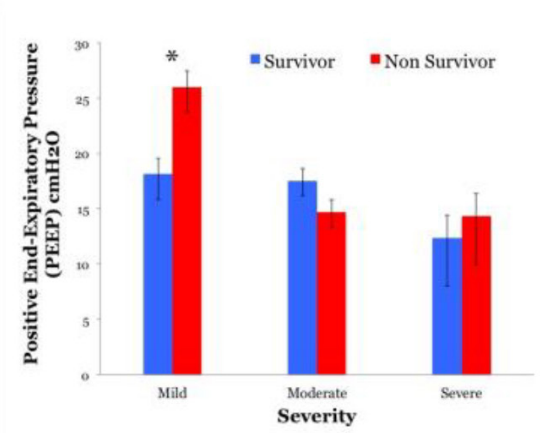

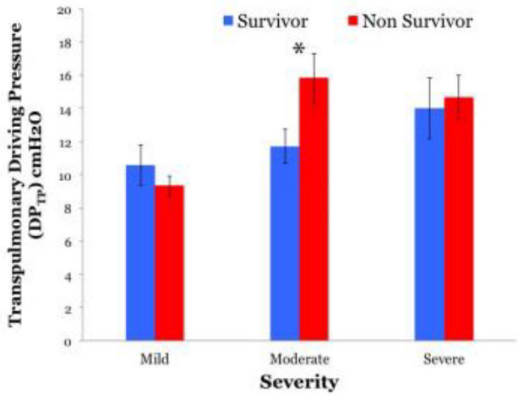

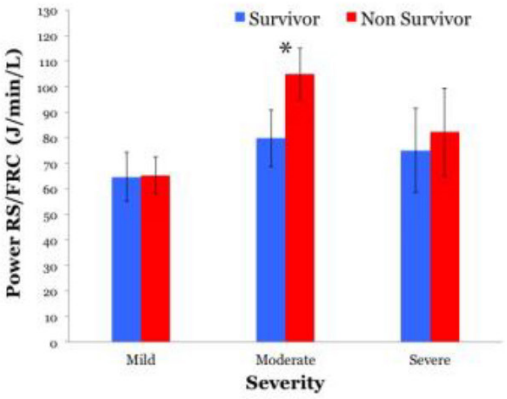

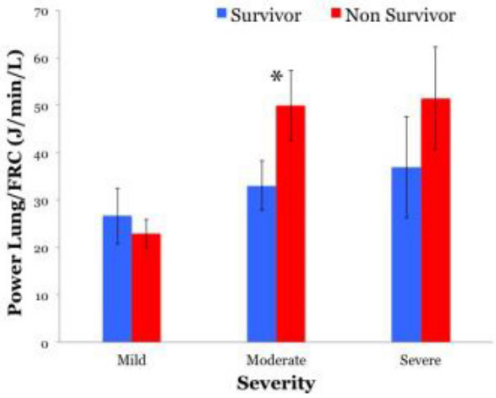

$$Mechanical\ Power_{RS} = 0{,}098 \times RR \times \Delta V \times \left(P_{Peak} - \frac{1}{2}(P_{Plat} - PEEP)\right)$$

$$Mechanical\ Power_{Lung} = 0{,}098 \times RR \times \left[\left(\frac{1}{2}\Delta V^2 \times EL_{Lung}\right) + \left(PEEP \times \frac{El_{Lung}}{EL_{RS}}\right) \times \Delta V\right]$$

$$FRC = \frac{EL_{spec} \times \Delta V}{\Delta P_{tp}}$$

Outcomes of Technology Dependent NICU Infants: A Single Center 5-Year Review Comparing Usual Care Versus Comprehensive Medical Care

De Jesus-Rojas W[1], Samuels CL[2], Eapen J[2], Gonzales T[2], Harris TS[2], McKay SL[2], Boricha F[2], Pedroza C[1], Aneji CU[3], McBeth K[1], Stark JM[1], Yadav A[1], Tyson JE[3], Mosquera RA[1]

[1]Division of Pulmonary Medicine/Allergy & Immunology/Rheumatology, Department of Pediatrics McGovern Medical School, University of Texas Health Science Center, Houston, Texas.
[2]High-Risk Children's Clinic, McGovern Medical School, University of Texas Health Science Center, Houston, Texas.
[3]Division of Neonatal-Perinatal Medicine, Department of Pediatrics, McGovern Medical School, University of Texas Health Science Center, Houston, Texas.

Background: Survival of premature infants has led to a growing population of technology-dependent children. Medical technology introduces additional complexity to patient care. Outcomes after NICU discharge comparing usual care (UC) with comprehensive care (CC) remain elusive.

Objective: To compare the outcomes of NICU infants discharged with tracheostomy following UC versus CC.

Methods: A single site retrospective study evaluated forty-three (N=43) NICU infants discharged with tracheostomy over 5-½ years (2011-2017). CC provided 24-hour accessible healthcare-providers using an enhanced-medical home. Mortality, total hospital admissions, 30-days readmission rate, time-to-mechanical ventilation liberation, and time-to-decannulation were compared between groups.

Results: CC group showed significantly lower mortality (3.4%) versus UC (35.7%), RR, 0.04 [95% CI, 0.002-0.85, P=0.03]. CC reduced total hospital admissions to 78 per 100 child-years versus 162 for UC; RR, 0.48 [95% CI, 0.25-0.93], P=0.03. The 30-day readmission rate was 21% compared to 36% in UC; RR, 0.58 [95% CI, 0.21-1.58], P=0.29). In competing-risk regression analysis (treating death as a competing-risk), hazard of having mechanical ventilation removal in CC was two times higher than UC; SHR, 2.19 [95% CI, 0.70-6.84]. There was no difference in time-to-decannulation between groups; SHR, 1.09 [95% CI, 0.37-3.15].

Conclusion: CC significantly decreased mortality, total number of hospital admissions and length of time-to-mechanical ventilation liberation.

Keywords: decannulation, tracheostomy, prematurity, technology-dependent children, mortality.

Auranofin, Thioredoxin Reductase Inhibitor in Lung Epithelial Cells Induces Heme Oxygenase-1 Via Nrf2-dependent Mechanisms

Katelyn Dunigan, Qian Li, Rui Li, Stephanie B. Wall, and Trent E. Tipple

Redox Biology Laboratory, Division of Neonatology, University of Alabama at Birmingham, Birmingham, Alabama

GThioredoxin reductase-1 (TrxR1) inhibition activates nuclear factor (erythroid-derived 2)-like 2 (Nrf2) and attenuates hyperoxic lung injury in neonatal and adult mice. Heme oxygenase-1 (HO-1) is regulated by Nrf2, although not exclusively. We have observed disproportionate increases in HO-1 levels following TrxR1 inhibition in vivo and in vitro; however, the role of Nrf2 in HO-1 induction by TrxR1 inhibitors is unclear.

Our studies tested the hypothesis that TrxR1 inhibition induces HO-1 via Nrf2-dependent mechanisms. Wild-type (WT) and Nrf2 knockout (KO) murine transformed club cells (mtCCs), generated using CRISPR/Cas9 gene editing, were treated with 0.5 μM of the TrxR1 inhibitor, auranofin (AFN), or control (DMSO) for 3h and lysates were collected. TrxR1 activity was measured determined by measuring insulin disulfide reductase activity. HO-1 mRNA and protein expression were determined by qRT-PCR and western blot, respectively. Data (n=5-6) were analyzed by 2-way ANOVA with Tukey's post hoc ($p<0.05$).

In KO mtCCs, baseline TrxR1 activity was 50% lower than that in WT cells. AFN treatment decreased TrxR1 activity by 50% when compared to respective control-treated WT and KO cells. To confirm that the KO mtCCs were able to generate Hmox1 and HO-1, WT and KO mtCCs were treated with hemin (5 μM), a Nrf2-independent HO-1 inducer, or DMSO control for 8h. In hemin-treated mtCCs, *Hmox1* levels were 5-fold greater than in control-treated cells. Hemin treatment increased HO-1 protein levels by 15-fold in WT and 5-fold in KO mtCCs when compared to respective control-treated cells. In AFN-treated WT mtCCs, Hmox1 levels were 30-fold greater than in WT controls. This corresponded with a 75-fold increase in HO-1 protein expression. Conversely, AFN treatment of KO cells increased Hmox1 levels by 2-fold. There were no differences in HO-1 protein expression between KO and WT mtCCs treated with AFN.

Our data suggest that Nrf2 is likely to be the primary pathway by which AFN increases HO-1 expression in mtCCs. HO-1 has been identified as a potential therapeutic target to prevent or treat acute lung injury. Future studies will investigate the role of Nrf2 in HO-1 induction in the lung in vivo and the contribution of HO-1 to the protective effects of TrxR1 inhibitors in our lung injury models.

MicroRNA Sequencing of Peripheral Blood Mononuclear Cells And Disease Staging and Severity in Sarcoidosis

N. Emeagwali[1], M. Vukmirovic[1], X. Yan1, K. F. Gibson[2], M. Gulati[1], G. Deluliis[1], T. Adams[1], B. Hu1, X. Li[1], A. Mihaljinec[1], S. O'Neal[2], M. Becich[2], H. Hochheiser[2], E. Herzog[1], E. S. Chen[3], A. M. Morris[2], J. K. Leader[2], Y. Zhang[2], J. G. Garcia[4], S. R. Wisniewski[2], P. V. Benos[2], L. A. Maier[5], D. R. Moller[3], K. Patterson[6], W. P. Drake[7], L. Koth[8], N. Kaminski[1]

[1]Section of Pulmonary, Critical Care and Sleep Medicine, Yale University School of Medicine, New Haven, CT, United States, [2]University of Pittsburgh, Pittsburgh, PA, United States, [3]Johns Hopkins University, Baltimore, MD, United States, [4]University of Arizona Health Sciences, Tucson, AZ, United States, [5]National Jewish Health, Denver, CO, United States, [6]University of Pennsylvania, Philadelphia, PA, United States, [7]Vanderbilt University, Nashville, TN, United States, [8]University of California San Francisco, San Francisco, CA, United States.

Rationale: MicroRNAs (miRNAs) are small non-coding RNAs that post-transcriptionally regulate the expression of thousands of genes in normal and disease states. We analyzed the miRNA profiles of peripheral blood mononuclear cells (PBMC) in a large cohort of well characterized sarcoidosis subjects by genome scale miRNA sequencing and correlated the miRNAs with scadding stage and disease severity.

Methods: PBMC were isolated from sarcoidosis subjects recruited in Genomic Research in Alpha-1 Antitrypsin Deficiency and Sarcoidosis study (GRADS) (Moller et al., Ann Am Thorac Soc, 2015 PMID: 26193069). RNA was extracted using Qiazol following Qiagen's miRNeasy protocol. After determination of RNA quality, cDNA libraries were prepared and sequenced by Ion Torrent Proton Sequencer with Ion PITM Chip which produced ~ 30 million single-end reads/sample with average read length of 150bps. Cufflinks was used to calculate Fragments per Kilobase of exon per Million (FPKM). miRNA's and genes that associated with phenotypes were identified using non-parametric correlation. Multiple hypothesis testing was addressed by controlling false discovery rate (FDR) < 0.05.

Results: 199 PBMC samples that passed quality control were used in this analysis. Those included 24 stage I, 33 stage II-III treated, 40 stage II-III untreated, 17 stage IV treated, and 12 stage IV untreated subjects. 53.2% were female and 23.1% were African American. There were several differentially expressed miRNAs in our samples some of which were associated with a reduction in lung function (FDR<0.05). Interestingly, miRNA 146b had a 5-fold increase in expression in untreated patients with scadding stage II-III disease compared with non-acute stage I (P<0.02). In addition, miRNA 365 had a 2-fold decrease in expression in untreated patients with scadding stage IV disease (P<0.03).

Conclusions: We identified miRNAs reflective of disease staging and severity in PBMCs, including miRNA 365, a negative regulator of IL-6, a pleiotropic cytokine involved in the inflammatory response, and miRNA 146b which correlates with the degree of fibrosis in myeloproliferative neoplasms. Continued miRNA analysis of this cohort will further elucidate the role of miRNAs in sarcoidosis.

Exploring the Provision of Primary and Specialty Palliative Care Services in Critically Ill Older Adults by Pre-Hospitality Frailty

O. Enilari[1], R. Nair[2], E. Chuang[3], M. N. Gong[4], A. A. Hope[4]

[1]Pulmonary and Critical Care , Montefiore Medical Center, Albert Einstein College of Medicine, Bronx, NY, United States, [2]Internal Medicine, Montefiore Medical Center, Bronx, NY, United States, [3]Family and Social Medicine, Palliative Care Service , Montefiore

Rationale: Older adults with pre-hospital frailty are at increased risk of morbidity and mortality. The provision of palliative care by frailty status in critically ill older adults has not been previously described, but may provide insight into ways to improve shared decision-making and communication in critically ill patients.

Methods: This is an observational cohort study of adults (age ≥ 50) admitted into Intensive Care Units (ICUs) across two hospitals within Montefiore Medical Center in Bronx, New York. Frailty was identified using the Clinical Frailty Scale, a judgment based frailty assessment tool previously validated in adult ICU patients. We abstracted from the medical record: (1) evidence of the completion of a specialty palliative care consultation (SPC), (2) the presence and development of seven evidence-based hospital process measures previously shown to be associated with a need for SPC in critically ill adults, (3) other markers of non-specialty or generalist palliative care (PPC) provision. We used descriptive statistics and logistic regression analyses to describe differences in palliative care provision by frailty status.

Results: In a cohort of 302 adults with age (mean ± standard deviation) (67.2 ±10.5), 50% (n=151) were identified as frail. Frail patients were not more likely to have one of the 7 triggers for SPC during their hospital stay (47.0% in frail patients versus 41.7% in non-frail, p=0.354). Of the 134 patients with one of the 7 triggers for SPC, only 55 (41.0%) had SPC during the hospitalization. Frail patients were more likely to have a SPC (31.8% in frail patients versus 17.9% in non-frail patients, p=0.005) and this effect was present even after adjusting for the presence of one of the 7 triggers for SPC (adjusted Odds Ratio (95% Confidence Interval) 2.1 (1.2-3.8), p=0.009). Of the 48 frail patients who had SPC, 15 (31.3%) did not have any of the 7 triggers for SPC. When SPC was completed in frail patients, the median (interquartile range) days to consultation was 16.5 (7-27.5). Furthermore, only in 56.3% of the frail patients did we find evidence of a family meeting documented in the chart by non-palliative care providers.

Conclusions: Among critically ill older adults, there are gaps in the provision of specialty and generalist palliative care consultation and more research should explore how frailty assessment should be integrated into the delivery of palliative care in the hospital setting.

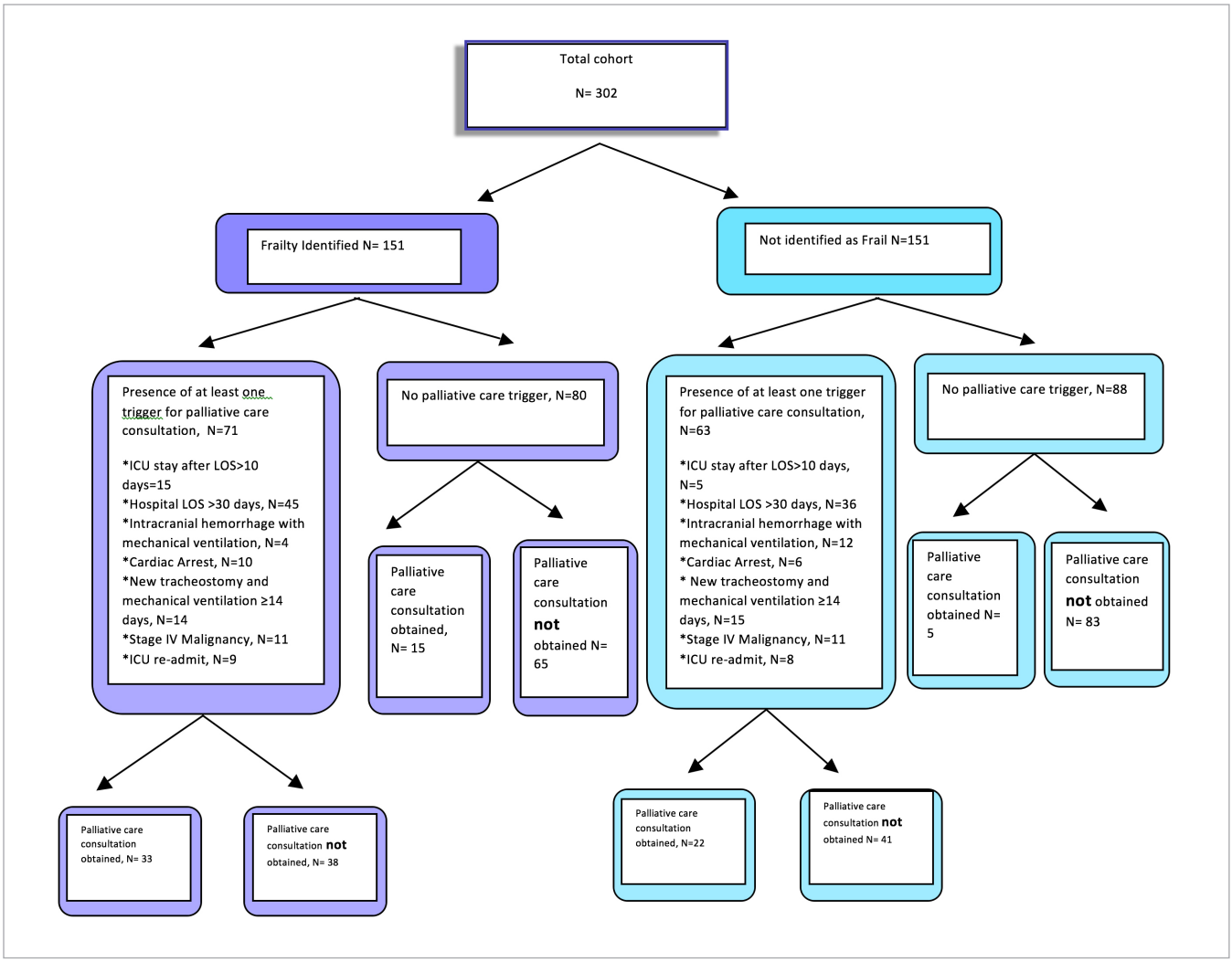
Total cohort
N= 302
Frailty Identified N= 151
Not identified as Frail N=151
Presence of at least one trigger for palliative care consultation, N=71
*ICU stay after LOS>10 days=15
*Hospital LOS >30 days, N=45
*Intracranial hemorrhage with mechanical ventilation, N=4
*Cardiac Arrest, N=10
*New tracheostomy and mechanical ventilation ≥14 days, N=14
*Stage IV Malignancy, N=11
*ICU re-admit, N=9
No palliative care trigger, N=80
Palliative care consultation obtained, N= 15
Palliative care consultation not obtained N= 65
Palliative care consultation obtained, N= 33
Palliative care consultation not obtained, N= 38
Presence of at least one trigger for palliative care consultation, N=63
*ICU stay after LOS>10 days, N=5
*Hospital LOS >30 days, N=36
*Intracranial hemorrhage with mechanical ventilation, N=12
*Cardiac Arrest, N=6
* New tracheostomy and mechanical ventilation ≥14 days, N=15
*Stage IV Malignancy, N=11
*ICU re-admit, N=8
No palliative care trigger, N=88
Palliative care consultation obtained N= 5
Palliative care consultation not obtained N= 83
Palliative care consultation obtained, N=22
Palliative care consultation not obtained N= 41

Bundled Consent in U.S. Intensive Care Units (ICUs)

M. L. Espinosa[1], A. Tannenbaum[2], M. Kilaru[3], J. Stevens[4], M. Siegler[5], M. D. Howell[6], W. F. Parker[7]

[1]University of Chicago Pritzker School of Medicine, Chicago, IL, United States, [2]Division of Pulmonary, Allergy, and Critical Care, Department of Medicine, Hospital of the University of Pennsylvania, Philadelphia, PA, United States, [3]Center for Healthcare Delivery Science & Innovation, UChicago Medicine, Chicago, IL, United States, [4]Center for Healthcare Delivery Science, Beth Israel Deaconess Medical Center, Boston, MA, United States, [5]MacLean Center for Clinical Medical Ethics, UChicago Medicine, Chicago, IL, United States, [6]Google Research, Mountain View, CA, United States, [7]Pulmonary and Critical Care, UChicago Medicine, Chicago, IL, United States.

Rationale: Bundled consent is the practice of obtaining anticipatory consent for a pre-defined set of common intensive care unit (ICU) procedures, such as central line and chest tube placement. In a controlled trial, bundled consent increased the number of procedures performed with consent without compromising patient/surrogate understanding, yet the adoption of this practice is unknown. We aimed to determine the national prevalence of bundled consent use in adult ICUs and its effect on acquiring consent for ICU procedures.

Methods: A nationally representative, random sample of U.S. hospitals with medical/surgical ICUs was selected from the American Hospital Association (AHA) guide. Surveyed ICU physicians and nurses reported whether they utilize bundled consent, the rate of obtaining consent prior to ICU procedures, and opinions about bundled consent. AHA data on hospital size, teaching affiliation, and staffing models were analyzed for differences by consent type. Propensity score nearest neighbor matching was used to adjust for baseline differences in hospitals by consent type.

Results: A total of 242 hospitals were reached and 65 completed the survey (27% response rate). There were no significant differences in hospital characteristics between responders and non-responders. The prevalence of bundled consent was 15% (95% CI 8%-26%). Bundled consent hospitals were larger than per-procedure hospitals with more total beds (median total beds 386 vs. 166, p = 0.065 by ranksum test) and ICU beds (median 28 vs 12 beds, p = 0.029) but were otherwise similar. The self-reported rate of "always" obtaining consent was 60% amongst bundled consent users and 27% amongst per-procedure users (unadjusted absolute difference 33%, 95% CI 25-65%). After well-balanced propensity score matching based on hospital and ICU size, the adjusted absolute difference in consent rate was 40% (95% CI 15%-65%). All bundled consent hospitals reported that they would recommend the practice to other hospitals. Common reasons why hospitals used bundled consent included preventing procedures done emergently without consent and efficiency for patients, surrogates, and providers. Forty-seven percent of per-procedure hospitals reported interest in implementing bundled consent.

Conclusions: In this cross-sectional nationally study of adult ICUs there was a low prevalence of bundled consent. Hospitals using bundled consent were over twice as likely to always obtain informed consent than traditional per-procedure consent hospitals. Bundled consent users have positive opinions of this consent protocol and always recommend it to other hospitals. Bundled consent may be an

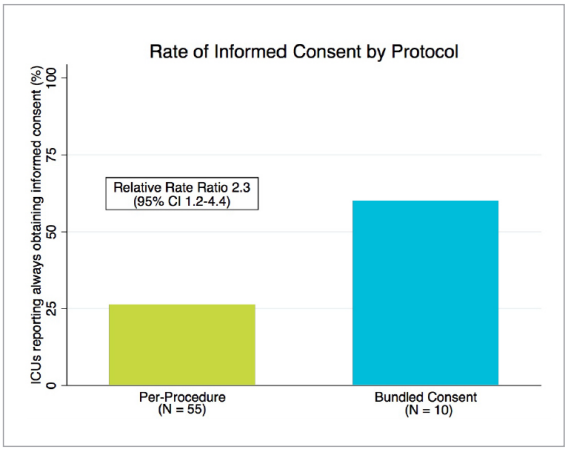

Sex-specific microRNA expression in ozone-induced lung inflammation

Nathalie Fuentes[1], Arpan Roy[1], Vikas Mishra[1], Noe Cabello[1], Susan DiAngelo[1], Judie Howrylak[2], and Patricia Silveyra[1]

[1]Department of Pediatrics, [2]Department of Medicine; The Pennsylvania State University College of Medicine, Hershey, Pennsylvania

Rationale: Sex differences in the incidence and prognosis of respiratory diseases have been reported. Studies have shown that women are at increased risk of adverse health outcomes from air pollution than men, but the specific mechanisms behind these differences have not been well studied. MicroRNAs (miRNAs) are environmentally sensitive posttranscriptional regulators of gene expression that may mediate the damaging effects of inhaled pollutants in the lung. Based on our preliminary data in which we found sex differences in the expression of lung inflammatory markers in response to ozone exposure, we hypothesized that sex-specific miRNA expression can mediate gender-specific immune responses to ozone via modulation of gene expression.

Methods: Male and female adult C57BL/6J mice were exposed to ozone (2ppm, 3h) or filtered air (FA, control). Four hours after exposure, whole lungs were harvested and RNA was extracted. We used PCR arrays to characterize sex-differences in the expression of 84 miRNAs predicted to regulate the expression of inflammatory genes in lung tissue. Results were analyzed with the limma package on R. Using false discovery rate adjustment for multiple comparisons and in silico ingenuity pathway analysis (IPA), we identified differentially expressed miRNAs in males and females in response to ozone, predicted target genes, and associated biological pathways.

Results: We identified basal and ozone-induced sex differences in lung miRNA expression. Exposure to ozone differentially affected lung miRNA expression in male and female mice. In silico analysis revealed that the top molecular functions associated with differentially expressed miRNAs in males vs. females exposed to ozone were linked to cell cycle, cellular development, and cellular growth and proliferation, which are important pathways in the lung inflammatory response. Moreover, the top associated network functions included organismal and tissue development, humoral immune response, and reproductive system development and function. Several differentially expressed miRNAs were also involved in inflammation (miR-130a-3p, miR-17-5p, miR-291a-3p and miR-338-5p), and their predicted targets are key regulators of the immune response (IL-6, SMAD2/3 and TMEM9).

Conclusions: We conclude that both sex and hormonal status can influence lung miRNA expression in response to ozone exposure. We postulate that sex-specific miRNA regulation of inflammatory gene expression may mediate differential health outcomes in men and women exposed to air pollution.

Influenza A-induced pneumonia accelerates aging-related cognitive decline in mouse models.

Francisco J. Gonzalez-Gonzalez, Alexandra C. McQuattie-Pimentel, Jennifer Yuan-Shih Hu, Ching-I Chen, Satoshi Watanabe, Dawn Bowdish, Alexander V. Misharin, Karen Ridge, G.R. Scott Budinger

Institution: Northwestern University

Rationale: The decline of cognitive function during aging is one of the most profound and debilitating limitations to health-span in elderly. To understand the mechanisms that underlie the age-related decline in cognition, most investigators have studied aged animals who have spent their lives shielded from environmental stress. Pneumonia represents a common and serious form of environmental stress that disproportionately affects older individuals. Elderly are at increased risk for bacterial and viral pneumonias, and suffer from a higher morbidity, mortality and number of complications when compared to younger individuals. There is a growing clinical and experimental evidence that viral and bacterial pneumonias lead to long-lasting declines in cognitive function. These findings suggest the presence of non-cell autonomous mechanisms linking pneumonia with cognitive decline.

Hypothesis: Age-related changes act synergistically with pneumonia to precipitate cognitive dysfunction in cell non-autonomous manner via activation of microglia.

Methods: Young (2 mo) and old (18 mo) C57Bl/6 mice intratracheally with a sublethal dose of influenza A virus (PR8). Cognitive and motor performance was assessed pre-infection, 2 weeks after the infection and 12 weeks after the infection using the panel of cognitive and behavioral tests. Transcriptional profiling of the frontal cortex and FACSorted microglia was performed via RNA-seq.

Results: Aged mice performed worse in cognitive (open field and novel object recognition test) and motor function tests (the rotarod and grip strength) than younger animals and that influenza A pneumonia had more pronounced effect on older than on younger mice: while young mice demonstrated almost complete recovery, the cognitive deficit persisted in older mice. Transcriptional profiling of the frontal cortex revealed that genes associated with axonogenesis, synapse formation, learning and memory were downregulated specifically in aged flu-treated mice. Transcriptional profiling of microglia revealed upregulation of the genes associated with unfolded protein response and response to proteostatic stress (*Atf3, Dnajb1, Hsp90ab1, Hspa8*), in young, but not in old mice, indicating disruption of this adaptive mechanism in aged microglia.

Conclusions: Our data demonstrate that aged mice are more susceptible to pneumonia-associated cognitive decline and indicate the role of cell-autonomous (aging-associated changes in microglia and cortex) and non-cell autonomous (lung injury) factors in this process.

MicroRNA-25 Modulates Proliferative Signaling via the Mammalian Target of Rapamycin Pathway in Asthmatic Airway Smooth Muscle Cells *In Vitro*

Miguel Hernandez, Mariam Ba, Karla Hernández, Eva Hernandez, Michelle Mendoza, Jon Evasovic and Cherie A. Singer

Pharmacology Department, University of Nevada, Reno School of Medicine, Reno, NV 89557

Rationale: Bioinformatic analyses predict that microRNA-25 (miR-25) targets the 3' untranslated region (UTR) of tuberous sclerosis complex 1 (TSC1), an upstream repressor of mammalian target of rapamycin complex 1 (mTORC1). Extensive studies in cancer cells have shown that rapamycin, an inhibitor of mTORC1, attenuates cell proliferation. Previous data from our lab establishes that miR-25 is down-regulated in airway smooth muscle (ASM) cells in vitro upon receiving a pro-inflammatory stimulus. Inhibition of miR-25 promotes ASM cell proliferation and correlates with enhanced Akt phosphorylation *in vitro*. Our laboratory has further demonstrated that miR-25 expression was inversely correlated with TSC1 transcript levels in the trachea of a mouse model of smooth muscle-targeted miR-25 expression (TgSM-miR25). Therefore, these experiments test the hypothesis that miR-25 targets TSC1 to attenuate ASM cell proliferation via mTOR signaling.

Methods: Asthmatic and non-asthmatic ASM cells were grown in culture. RNA and protein were extracted from proliferating, 2-day and 7-day growth arrested cells. The role of miR-25 expression on TSC1, mTORC1 and S6 Kinase, a downstream effector of the mTOR pathway, was assessed via qPCR and western blot analyses.

Results: Expression of miR-25 was down-regulated by ~70% in proliferating asthmatic ASM cells, and inversely correlated with TSC1 mRNA and protein levels. Phosphorylation of mTOR (p. mTOR) at the serine-2448 (Ser-2448) repressor site was reduced in asthmatic ASM cells, while P70S6K phosphorylation was increased in proliferating and 7-day growth arrested asthmatic ASM cells. There was also reduced Raptor expression in asthmatic ASM cells, indicative of increased mTORC1 activity in asthmatic ASM cells.

Conclusions: Together, these data suggest that mTOR activity is augmented in asthmatic airway ASM cells due to reduced Ser-2448 phosphorylation. The steady P70S6K phosphorylation levels between 7-day growth arrested asthmatic ASM cells and proliferating control supports the idea that not all asthmatic ASM cells reach mature differentiated phenotype, and remain in a proliferative state. Further experiments will test effect of miR-25 expression on the mTORC1 signaling pathway. These studies will clarify the role of miR-25 on proliferative targets during asthma pathogenesis, advancing the establishment of miR-25 as a novel therapeutic candidate for asthma.

Funding sources: This study is supported by R01 HL127192-01A1 and 3R01HL127192-02W1 from the NHLBI to CAS.

Cleaved RAGE is the Predominant Early-Evoked sRAGE Isoform and Confers Risk for Sepsis-Associated ARDS

Jones TK[1], Feng R[1], Reilly JP[1], Johansson, ED[1], Dunn TG[1], Ittner CAG[1], Anderson BJ[1], Shashaty MG[1], Christie JD[1], Meyer NJ[1]

[1]University of Pennsylvania, Philadelphia, PA

Rationale: Plasma levels of the soluble receptor for advanced glycation end products (sRAGE) strongly associate with Acute Respiratory Distress Syndrome (ARDS), and sRAGE has been implicated as a potential causal intermediate in ARDS. Plasma sRAGE consists of two primary implicated as a potential causal intermediate in ARDS. Plasma sRAGE consists of two primary isoforms, endogenous secretory RAGE (esRAGE) and cleaved RAGE (cRAGE), which are generated by distinct mechanistic pathways. However, it is unknown which isoform contributes to ARDS risk. We used a genetic instrumental variable technique, Mendelian Randomization (MR), to determine if plasma sRAGE isoforms in sepsis are genetically regulated and associated with risk of ARDS.

Methods: We enrolled 171 critically ill patients with sepsis and measured plasma sRAGE and plasma esRAGE concentrations by ELISA on ED admission. We calculated plasma cRAGE by subtracting esRAGE from sRAGE concentrations. Patients were genotyped using an Affymetrix Tx v1 array and were followed for 6 days for ARDS per Berlin criteria. We used multivariable logistic regression to test the association between the sRAGE isoforms and ARDS adjusting for confounders. For MR, we selected the top 20 single nucleotide polymorphisms (SNPs) strongly associated with sRAGE concentrations as the genetic instrument. The causal effects of sRAGE, cRAGE, and esRAGE were estimated using an inverse-variance weighted MR model based on the genetic instrument adjusting for age, sex, genetic ancestry, and pulmonary source of infection.

Results: Plasma sRAGE was strongly associated with ARDS, with an adjusted odds ratio of 2.02 per log increase (95% CI [1.30, 3.14]; p=0.002). Plasma cRAGE accounted for on average 2.02 per log increase (95% CI [1.30, 3.14]; p=0.002). Plasma cRAGE accounted for on average ARDS; adjusted OR 2.40 (95% CI [1.51, 2.78]; p<0.001) and 1.65 (95% CI [0.97, 2.81]; p=0.06), respectively. The two sRAGE isoforms were strongly correlated (r=0.73, p<0.001). In the causal effect model, a unit increase in log-transformed cRAGE was significantly associated with a 3.8% (95% CI [0.3%, 7.2%]) increase in ARDS risk (p=0.03) whereas a unit increase in esRAGE was (95% CI [0.3%, 7.2%]) increase in ARDS risk (p=0.03) whereas a unit increase in esRAGE was not significantly associated with ARDS risk (-3.0%, 95%CI [-7.1%, 1.1%], p=0.15).

Conclusions: In sepsis-associated ARDS, cRAGE is the predominant early-evoked sRAGE isoform. Both esRAGE and cRAGE isoforms demonstrate genetic regulation and associate with ARDS, although only cRAGE achieved statistical significance for a causal effect between the genetic variants and ARDS risk. Our findings indicate that both isoforms may contribute to ARDS risk, and additional investigations into sRAGE with an emphasis on the cleaved isoform may elucidate novel intervenable targets for ARDS therapy.

Facial Phenotype in Children and Young Adults with Rapid-onset Obesity with Hypothalamic dysfunction, Hypoventilation, and Autonomic Dysregulation (ROHHAD): Quantitative Pattern of Dysmorphology

Leslie Martinez[1,3], Amy Zhou, BA[1,3], Emma Dunne[1,3], Casey M Rand, BS[1,3], Helen Binns, MD, MPH[2,3,4], Debra E Weese-Mayer, MD[1,2,5]

Ann & Robert H. Lurie Children's Hospital of Chicago, Department of Pediatrics, [1]Division of Pediatric Autonomic Medicine, [2]Center on Obesity Management and Prevention [3]Stanley Manne Children's Research Institute, Northwestern University Feinberg School of Medicine, [4]Department of Preventative Medicine and [5]Pediatric Autonomic Medicine, Chicago, IL, United States

Introduction and Rationale: ROHHAD is an extremely rare, life-threatening neurocristopathy with a hallmark presentation of rapid-onset weight gain (20-30 lbs) over 6-12 months after 1.5 years of age. The etiology of ROHHAD is unknown, and early stages may be difficult to distinguish from sleep apnea/exogenous obesity. Delayed diagnosis can lead to increased risk of morbidity/mortality from unrecognized hypoventilation. A typical ROHHAD facial phenotype has been clinically observed, but not previously objectively evaluated. We hypothesized that objective facial anthropometric measurements from digital photos would reveal a ROHHAD-specific facial phenotype that might expedite identification of ROHHAD.

Methods: Subjects included 12 clinically confirmed ROHHAD patients and BMI- and gender-matched controls. Digital facial photographs (frontal and lateral views) at rest (non-smiling) were obtained with a horizontal ruler held at root of neck to ensure scale. Linear measurements were made using Inkscape software. Indices of computed ratios were calculated and presence/absence of "lip trait" (inferior inflexion of the lateral one-third of the upper vermillion border is flesh-colored instead of pink) was determined.

Results: Univariate analysis of continuous variables using the non-parametric Wilcoxon signed rank test are provided in Table 1. Five continuous variables differed significantly between ROHHAD and controls. Additionally, the "lip trait" was present in 91.7% of ROHHAD cases and 8.3% of controls

($p<0.001$).

Conclusions: This is the first study to examine the facial phenotype in ROHHAD. By comparing ROHHAD cases to BMI-matched controls we effectively isolated the impact of obesity on facial phenotype. ROHHAD faces were generally shorter and flatter with a characteristic "lip trait", confirming the differences observed clinically. Results indicate the potential of using facial photogrammetry as an objective diagnostic tool in ROHHAD. Such a tool might enable earlier identification of ROHHAD and conservative management before significant disease progression, onset of hypoventilation, and risk for life-threatening morbidity and mortality. The measures identified here should be integrated into a predictive model by testing on a separate case-control cohort. The results of this study are similar to those previously identified in Congenital Central Hypoventilation Syndrome (CCHS), a neurocristopathy with early embryologic origins and disordered breathing similar to that found in ROHHAD. These findings indicate the possibility of a similar etiology for ROHHAD.

The function of endothelial TRPV4 channels is attenuated in pulmonary arterial hypertension

Corina Marziano, Kwangseok Hong, Eric L. Cope, Swapnil K. Sonkusare

Rationale: The endothelium is an important regulator of pulmonary vascular resistance. Endothelial dysfunction is a major contributor to increased pulmonary vasoconstriction and elevated pulmonary arterial pressure (PAP) in pulmonary arterial hypertension (PAH). We recently identified TRPV4 (transient receptor potential vanilloid 4) channels as an important Ca2+ entry pathway in the intact endothelium from small, resistance-sized PAs, and demonstrated that TRPV4 channels regulate the activity of endothelial nitric oxide synthase (eNOS) and endothelium-dependent vasodilation of small PAs. NO bioavailability is reduced in PAs from PAH patients and mouse models of PAH. However, the pathological mechanism for reduced NO bioavailability in PAH are not clear. We hypothesized that perturbations of endothelial TRPV4 channel function contribute to reduced NO bioavailability and loss of endothelium-dependent vasodilation in PAH.

Methods: Three-week chronic hypoxia (CH) and Sugen 5416 + CH models were used to induce PAH in mice. TRPV4 channel function was studied using novel "optical patch clamp" approach that uses high-speed Ca2+ imaging to record single TRPV4 channel function ("TRPV4 sparklets") in the intact endothelium from small, resistance-sized PAs. Pressure myography in small PAs was used to investigate the functional consequence of TRPV4 channel activation. Right ventricular systolic pressure (RVSP) was measured as an indicator of PAP. DAF-FM diacetate was used to measure changes in NO in the intact artery.

Results: In the CH model of PAH, TRPV4-/- mice showed exacerbated increase in RVSP when compared to wild-type control mice, supporting the role of TRPV4 channels as important regulators of PAP. In arteries obtained from CH or Sugen 5416 + CH mice, endothelial TRPV4 sparklet activity was significantly reduced and TRPV4-mediated vasodilation was drastically lower compared to normoxic control mice. The expression of TRPV4 channels at mRNA level and TRPV4 immunofluorescence in the endothelium were not altered in PAs from CH or Sugen 5416 + CH models of PAH, suggesting altered TRPV4 channel regulation, not altered expression, in PAH. Moreover, TRPV4-induced NO release was impaired in the PAs from PAH mice.

Conclusions: Reduced TRPV4 channel function may contribute to decreased NO bioavailability and loss of endothelium-dependent vasodilation in PAH. Targeting the mechanisms that impair TRPV4 channel function in PAH may lead to novel therapeutic strategies.

The Impacts of Particulate Pollution on Acute Pulmonary Exacerbations, FEV1, and FVC in Cystic Fibrosis Patients

Daniel L. Mendoza, PhD, Cheryl S. Pirozzi, MD MS, Theodore G. Liou, MD, Nicole Harlan, MD, Robert Paine MD

Division of Pulmonary Medicine, University of Utah School of Medicine

Rationale: Acute pulmonary exacerbations (APE) are critical events in the progression of lung disease in patients with cystic fibrosis. The precipitating events for APE are poorly understood. We aimed to determine whether short-term exposure to fine particulate matter (PM2.5) was associated with APE and decline in lung function in CF patients. The Wasatch Front, a highly urbanized region housing approximately 80% of Utah's population and cystic fibrosis (CF) patients, is bounded by mountains in the east and west. This topography contributes to episodic pollution events in the setting of wintertime atmospheric inversions and summertime wildfires..

Methods: We studied patients with confirmed CF who produced sputum and were enrolled during clinical stability for an observational study seeking sputum biomarkers predictive of future acute pulmonary exacerbations. Study patients lived in six air quality measurement basins. We estimated PM2.5 exposure for each patient based on home address using the spherical kriging semivariogram method. We calculated the mean PM2.5 concentrations for each week during the study period. We used weekly median concentrations to categorize each week as either a "high" or "low" pollution week. We counted APEs that occurred during high or low pollution weeks and calculated mean and maximum cumulative pollution exposure levels for 1, 3, 7, 14, 21, and 28 days preceding each APE. We compared pollution levels at each lag step to the annual average PM2.5 exposure concentrations for each patient. We also compared patient spirometry to PM2.5 levels at the time of and preceding each day of measurement.

Results: The APEs (N=36) were associated with the weeks of high PM2.5 concentrations ($p = 0.045$). There was a trend towards association of APE with a week of high PM2.5 concentrations preceding the event ($p = 0.096$). The lagged mean concentrations preceding an event were not higher than the annual mean concentrations for any lag period ($p > 0.6$). Neither FEV1, FEV1%, FVC, nor FVC% showed any relationship with lagged mean concentrations of PM2.5 ($r2 < 0.06$).

Conclusions: This pilot study suggests an association between particulate air pollution and APEs in our CF population. Comparisons of lagged cumulative PM2.5 exposure against yearly averaged PM2.5 exposure as a predictor of APEs or spirometry test results were inconclusive. Further study with a larger sample size and further analysis of spirometry data is our proposed next step.

Sex Differences in Pulmonary Exacerbations in CF

K. Montemayor[1], R. Dezube[1], N. Lechtzin[1], M. Jennings[1], A. Thaxton[1], S. Allgood[1], C. Merlo[1], K. Riekert[1], N. West[1]

[1]Johns Hopkins University, Baltimore, MD

Rationale: Cystic fibrosis (CF) is a genetic disorder that affects more than 70,000 individuals worldwide, and results in repeated pulmonary exacerbations (PEx), leading to decreased lung function, quality of life, and survival. PEx can lead to permanent loss of lung function with risk factors including failing initial treatment with oral antibiotics, treatment location (home versus hospital) and shorter duration (<9 days) of intravenous (IV) antibiotics. Women with CF have decreased survival, but the reasons are unclear. There have been limited studies evaluating the existence of sex differences in frequency, treatment, and outcomes in PEx. Thus, sex differences related to PEx is important to clarify to help address this sex disparity.

Methods: We extracted data from the Cystic Fibrosis Foundation Patient Registry (CFFPR) for patients seen at the Johns Hopkins Adult CF center between June 2016 through June 2017. Variables included sex, frequency of PEx, duration of IV antibiotics, treatment location, and severity of PEx. PEx were defined as a physician's decision to treat symptoms and/or drop in lung function with oral or intravenous (IV) antibiotics. PEx were characterized in the CFFPR as mild (mild increase in symptoms treated with oral or inhaled antibiotics), moderate (clinically significant increase in symptoms treated with oral or inhaled antibiotics), and severe (clinically significant increase in symptoms requiring IV antibiotics).

Results: We identified 142 women and 153 men during this study period (total 295). Women had a higher frequency of PEx at 82 events (57.7%) versus men at 65 events (42.5%), p=0.009. There was a trend with women spending less time in the hospital (44%) compared to men (55%), though not statistically significant (p=0.14). There was a trend of more women (24%) being treated solely at home with IVs compared to men (17%) (p=0.15). Among the patients who had exacerbations, the average duration of treatment for a PEx was 15.1(SD 6.5) days for women compared to 14.5 (SD 7.8) days for men (p=0.46). The breakdown of severity of PEx was similar between groups.

Conclusions: In our single-center cohort study, women had a statistically significant higher percentage of PEx. There was a trend towards less time spent in the hospital for treatment of PEx, which can be associated with worse outcomes. It is unclear why women have decreased survival in CF, and these findings suggest increased frequency of PEx and different treatment patterns may contribute to worse outcomes in women.

Development of an Automated Metered Dose Inhaler to Deliver Fluticasone to Rats and Examine the Effects of Corticosteroids on Upper Airway Function and Structure

N. Morel[1], O. Broytman[1], J. Martinez[2], M. Teodorescu[1]

[1]Medicine, University of Wisconsin School of Medicine and Public Health, Madison, WI, United States, [2]Information Technology Academy, University of Wisconsin, Madison, WI, United States

Introduction: Obstructive Sleep Apnea (OSA) is more common among patients with asthma and inhaled corticosteroid usage may be a reason. Corticosteroids have been shown to cause myopathy of skeletal muscles. Herein, we are developing a rat model to test this effect on upper-airway muscles' function and structure. We are developing an MDI device to deliver Fluticasone automatically when a rat bites the MDI mouthpiece.

Methods: After priming a Fluticasone Metered Dose Inhaler (MDI) 220 mcg/puff, a 10G oral gavage needle was attached to its opening to deliver the medication in a smaller radius, more appropriate for a rat mouth. A device is currently being built to automatically actuate the MDI when the rat bites on this needle. A separate, unmodified MDI was used as the comparator for the unmodified inhaler trials. As a first step, we tested the efficiency of this model by weighing the amount of medication dispensed in four trials, and comparing it to that dispensed from an unmodified inhaler. In each trial, powder from five consecutive actuations was captured on an adhesive surface and weighed with an electronic scale. During the trials, we observed deposition of drug: in the unmodified inhaler, leftover powder could be seen around the inside of the mouthpiece; in the modified inhaler, drug was deposited on the external needle surface at the point of attachment to the MDI, as well as inside the needle. Data were analyzed in Excel. A two-tailed heteroscedastic t-test was used to determine differences between the two delivery methods. Efficiency of the modified inhaler was calculated by dividing its mean by the mean delivery from the unmodified inhaler.

Results: The Table below presents means of all actuations for each trial, followed by the overall mean, standard deviation and standard error of the mean for each method. Compared to the unmodified MDI version, our modified rat inhaler's efficiency rate was calculated at 46.2%.

Conclusions: The current version of our system delivers inhaled medication to the rat at approximately half efficiency to the unmodified MDI. Steps to further optimize it, including sealing around the needle connection to the MDI, assessment of electrostatic properties and changing to a needle of a plastic material or lubricating the current one's inner surface are currently undertaken.

	Unmodified Inhaler	Modified (Rat) Inhaler
Trial 1	125 mcg	120 mcg
Trial 2	220 mcg	120 mcg
Trial 3	220 mcg	60 mcg
Trial 4	300 mcg	100 mcg
Mean	216.25 mcg	100 mcg
Standard Deviation	71.6	28.3
Standard Error of the Mean	35.8	14.1
Efficiency		46.2%
T-Test, p-value	0.02	

Endothelial Autophafy is Necessary for Tumor Angiogenesis and Tumor Growth

C. D. Ochoa, G. Fu, R. Wu, C. Liao, L. S. Terada

Division of Pulmonary and Critical Care, Department of Internal Medicine, University of Texas Southwestern Medical Center, Dallas, TX, United States

Background: Lung cancer remains the most common cause of cancer-related deaths worldwide. Lung cancer growth, invasion, and metastasis are contingent on angiogenesis; however, current anti-angiogenesis therapies offer dramatic but short-lived effects on tumor growth and are limited by systemic side effects. Thus, the discovery of novel therapeutic targets that are effective and specific against tumor angiogenesis is of the utmost necessity. Autophagy is a conserved evolutionary process by which the cell sequesters damaged macromolecules and organelles into autophagosomes and delivers them to lysosomes for degradation and recycling. Autophagy is linked to tumor development, but its role is complex and incompletely understood. More specifically, endothelial autophagy's role in lung tumor angiogenesis is largely unknown.

Methods: To address this gap in knowledge, we engineered a mouse model of defective endothelial autophagy by knocking out the autophagy-essential gene *Atg5* specifically in endothelium. We crossed $Atg5^{fl/fl}$ mice, harboring a floxed *Atg5* exon 3, with VE-cadherin-Cre mice, both on C57BL/6 backgrounds. This generated $Atg5^{fl/fl}$;VE-Cre ($Atg5^{fl/fl}$) and $Atg5^{+/fl}$;VE-Cre ($Atg5^{+/fl}$) animals. We examined tumor angiogenesis by heterotopic implantation of Lewis Lung Carcinoma 1 (LLC1) cells in the right flank of both $Atg5^{fl/fl}$ and $Atg5^{+/fl}$ mice. After 21 days, tumors were resected, and tumor weight and tumor growth rates were determined. Malignancies were subsequently evaluated for vessel density and vessel maturity following the established immunohistochemistry protocols. As Collagen I is not present in normal basement membranes but is expressed by lung cancers among other tumors, we next investigated lung endothelial Collagen I matrix invasion. Finally, we tested the lung endothelial secretion of angiogenic factors including IL-6, a known modulator of pathological angiogenesis.

Results: First, adult Atg5fl/fl were phenotypically normal. Second - interestingly - at 21 days post-implantation, LLC1 tumor weight was decreased, and tumor growth rate was blunted in Atg5fl/fl mice when compared to $Atg5^{+/fl}$ controls. Third, tumor microvascular density was reduced in $Atg5^{fl/fl}$ mice when compared to $Atg5^{+/fl}$ littermates. Fourth, albeit the reduced angiogenesis, $Atg5^{fl/fl}$ tumor vessels displayed higher pericyte association indicating greater maturity. Fifth, isolated primary *Atg5*fl/fl lung endothelial cells demonstrated loss of invasion into Collagen I matrices when compared to *Atg5*+/fl mice. And sixth, $Atg5^{fl/fl}$ lung endothelial cells secreted less IL-6 when grown in Collagen I coated plates.

Conclusions: Endothelial autophagy is not required for normal vascular homeostasis. However, tumors need endothelial autophagy for angiogenesis and growth. Additionally, autophagy is necessary for lung endothelial cell secretion of IL-6 and invasion of Collagen I matrices.

NRF2 Regulation of ADH7 Expression in the Human Airway Epithelium Occurs via both Retinoic Acid Receptor and KEAP1 Pathways

S. Owusu, G. Wang, P. L. Leopold, J. Salit, R. G. Crystal

Weill Cornell Medical College, New York, NY, United States

Rationale: Retinoic acid (RA), a critical compound in lung regeneration and repair, is generated in lung cells by a series of oxidative reactions that convert dietary Vitamin A (retinyl palmitate) to RA. Alcohol dehydrogenase 7 (ADH7), a gene markedly upregulated in the human airway epithelium in response to oxidative stress, plays a role by catalyzing the rate limiting step in RA synthesis (conversion of retinol to retinal). Based on the knowledge that the ADH7 promoter contains an antioxidant response element that binds to nuclear factor erythroid 2-related factor 2 (NRF2), an oxidant (and hence cigarette smoke) response transcription factor, and the importance of ADH7 in providing sufficient RA to lung epithelial cells, we asked: does NRF2 play a central role in regulating ADH7 expression in human airway epithelium?.

Methods: The role of NRF2 in modulating ADH7 expression was assessed in primary normal human airway basal stem/progenitor cells differentiating to a mucociliary epithelium on an air liquid interface (ALI) culture. Three approaches were used including assessment of: (1) the effect of RA levels on ADH7 levels; (2) the effect of inhibition of the RA receptor (RAR) on ADH7 levels; and (3) the effect of siRNA-mediated knockdown of Kelch-like erythroid cell-derived protein 1 (KEAP1), an NRF2 antagonist, on ADH7 levels.

Results: Using the ALI model, quantitative PCR analysis demonstrated an inverse dose-response relationship between the concentration of RA (10-200 nM) at the time of establishment of ALI culture and ADH7 transcript levels, with 200 nM RA inducing a 2.6-fold decrease. BMS 493 (1 μM), a RAR inhibitor, resulted in a 1.8-fold increase in ADH7 mRNA levels. Knockdown of the constitutive NRF2 inhibitor, KEAP1, led to a 3.1±0.38-fold increase in ADH7 mRNA levels ($p<0.0001$). In each case, HMOX1 (a prototypical NRF2-regulated gene) transcription levels changed in a manner comparable to ADH7.

Conclusions: Taken together, the data suggest that NRF2 regulates ADH7 transcript levels via both RA/RAR and KEAP1 pathways. This mechanism likely contributes to the ADH7 transcriptional response to cigarette smoke in human airway epithelial cells, with NRF2 participating in a RA feedback loop to regulate ADH7 expression.

Matters of Mucus: Mucociliary Physiology in a Bleomycin-Induced Pulmonary Fibrosis Ferret

Jacelyn E. Peabody[1,2,3], Scott E. Phillips PhD[3], Vivian Y. Lin1, Jeremie M. Lever[2,3], Ren-Jay Shei PhD[1,3], Denise Stanford[3], John Engelhardt PhD[4], Trenton R. Schoebe DVM PhD[3], Corinne Hennessy[5], Evgenia Dobrinskikh PhD[5], Guillermo J Tearney MD PhD[6], David A. Schwartz MD[5], Steven M. Rowe MD, MSPH[1,3]

[1]Cystic Fibrosis Research Center, Department of Medicine, University of Alabama at Birmingham, Birmingham, Alabama, [2]Medical Scientist Training Program, School of Medicine, University of Alabama at Birmingham, Birmingham, Alabama, [3]Department of Medicine, University of Alabama at Birmingham, Birmingham, Alabama, [4]Department of Medicine, University of Iowa, Iowa City, Iowa, [5]Department of Medicine, University of Colorado Anschutz Medical Campus, Denver, Colorado, [6]Wellman Center for Photomedicine, Massachusetts General Hospital, Boston, Massachusetts

Introduction: Idiopathic pulmonary fibrosis (IPF) is a progressive fibrotic lung disease with median-survival ranging from 3-5 years after diagnosis. The greatest risk factor for developing IPF is a gain-of-function promoter variant in the mucin MUC5B; however, the role of MUC5B in IPF pathogenesis is unknown. Unlike rodent IPF models, ferrets airways contain submucosal glands, the major source of MUC5B in humans. We are developing a novel bleomycin-induced pulmonary fibrosis ferret model to evaluate the hypothesis that mucociliary physiology may alter pro-fibrotic mechanisms.

Methods: A single-dose of bleomycin-sulfate solution (2.5-5U/kg) or saline-vehicle was administered intratracheally via microaerosolization to normal ferrets. Fibrosis was assessed with μCT scans, histology, and second harmonic imaging. Functional microanatomy of the airway epithelium including airway surface morphology, ciliary beating (CBF), and mucociliary transport (MCT) were assessed ex-vivo using micro-optical coherence tomography (μOCT). Muc5B expression was assessed with immunohistochemistry.

Results: All ferrets (N=16) survived to euthanasia at 3 or 6 weeks post-bleomycin administration. μCT scans demonstrated evidence of patchy airway-centric and peripheral ground glass opacities that was worse in the dependent lung, evident at 2 weeks, and persistent through 6 weeks. Threshold-based volumetric μCT analysis revealed that bleomycin-treated lungs showed 38.2% fibrosis and a significant increase from baseline compared to controls (mean increase 18.1±2.2% bleomycin compared to -0.8±0.8% control, $P<0.001$). Histopathological analysis revealed airway centric inflammatory infiltrates, patchy severe interstitial fibrosis with cystic remodeling and epithelialization, airway remodeling, diffuse alveolar damage, type II pneumocyte hyperplasia, and pleural thickening. Second harmonic imaging revealed dose-dependent fibrosis with 3.35±0.1 and 5.41±0.57 mean intensity for 2.5U/kg and 5U/kg bleomycin ferrets, respectively ($P<0.05$). Masson's trichrome staining revealed distinct regions of fibroblasts and collagen matrix, resembling fibroblastic foci observed in humans. Proximal and distal airways had goblet cell hyperplasia with increased Muc5b staining. Immunohistochemistry for Muc5b was also observed in cystic areas of metaplastic epithelization. Evaluation of mucociliary transport by μOCT (N=4/group) following carbachol stimulation showed decreased MCT in bleomycin-treated main-stem bronchi (0.2±0.1mm/min) compared to controls (3.4±2.0 mm/min, $P=0.10$). Bleomycin treated ferrets also had reduced CBF in the main-stem bronchi (8.8±0.3 Hz, $P=0.057$) prior to carbachol compared to controls (10.7±0.6 Hz, respectively).

Conclusions: Bleomycin treatment induced pulmonary fibrosis in ferrets, with inflammation, fibrotic lesions, and remodeling changes analogous to IPF in humans. Contemporaneous analysis of fibrosis development and the mucociliary transport apparatus suggests a strong relationship and indicates that the altered airway surface microenvironment may affect the pathogenesis of fibrosis.

Comparison of Biomarkers of Inflammation and Immune Status in the Nose, Central Airways, and Serum of E-Cigarette Users and Cigarette Smokers

Alexia Perryman[1], Jessica Hoffman[2], Meghan E. Rebuli[1], Neil E. Alexis[3,4], Ilona Jaspers[1,3,4]

[1]Curriculum in Toxicology, UNC Chapel Hill, [2]Curriculum for the Environment and Ecology, UNC Chapel Hill, [3]Center for Environmental Medicine, Asthma, and Lung Biology, UNC Chapel Hill, [4]Department of Pediatrics, UNC Chapel Hill

Rationale: E-cigarette use has rapidly increased due to its promotion as a safer alternative to traditional tobacco products and its popularity among never smokers, especially young adults. While cigarette smoke exposure has been demonstrated to have inflammatory and immunosuppressive effects within the airways, the effects of e-cigarette use remain unclear. Our lab has previously shown that e-cigarette use is associated with greater down-regulation of RNA expression for immune-related genes in nasal epithelial cells as compared to cigarette smoking. In addition, e-cigarette use has been shown to be associated with elevated levels of markers of neutrophil activation and mucins in sputum. However, less is known about the effects of e-cigarette use on the comparative levels of inflammatory mediators throughout the respiratory tract and in systemic circulation.

Methods: In this study, we generated cytokine profiles for cigarette smokers (n=10), e-cigarette users (n=10), and non-smokers (n=10) using biological specimens collected from the upper and central respiratory tract and systemic circulation. We collected matched samples of epithelial lining fluid (ELF) from the nasal mucosa, nasal lavage fluid (NLF), induced sputum, and serum from healthy volunteers. Smoking category was assessed using self-reported cigarette/e-cigarette use and serum cotinine and urine NNAL levels. Cytokine levels were analyzed by multiplex ELISA. Data were compared across the biological specimens and smoking groups by two-way ANOVA and correlations between specimens determined by linear regression. To adjust for variable dilutions of the biological specimens, the prevalence of cytokines in each biological specimen was ranked.

Results: ELF and NLF showed a strong correlation; however, this correlation was driven by the prevalence of different cytokines in each specimen. A comparison of the ranked analytes revealed ELF and sputum clustered together, NLF clustered alone, and serum did not correlate with any of the respiratory specimens. TARC was found to be elevated in the serum of cigarette smokers, but not e-cigarette users. Interferon-inducible chemokines, such as MIG/CXCL9 or I-TAC/CXCL11, were suppressed in e-cigarette users in ELF, NLF, and induced sputum, but only MIG was found to also be suppressed in serum. When stratified by sex, cytokine profiles clustered more closely based on smoking group.

Conclusions: Our results suggest that ELF may serve as a better predictor of innate immune status in the lower airways than NLF. Furthermore, decreased expression of immune-orchestrating chemokines such as I-TAC/CXCL11 and MIG/CXCL9, may be indicative of e-cigarette-induced immunosuppressive effects. To better ascertain effects of e-cigarette use, sex differences may need to be considered.

Health Insurance and Disparities in Mortality Among Older Survivors of Critical Illness

Yoland Philpotts, MD[1]; Xiaoyue Ma, MS[2]; Michaela R Anderson, MD[1]; May Hua, MD, MS[2,3]; Matthew Baldwin, MD, MS[1]

[1]Division of Pulmonary, Allergy and Critical Care, Department of Medicine, Columbia University College of Physicians & Surgeons, New York, NY; [2]Department of Anesthesiology, Columbia University College of Physicians & Surgeons, New York, NY; [3]Department of Epidemiology, Mailman School of Public Heath, Columbia University, New York, NY.

Rationale: Access to care and outcomes for several diseases have been shown to differ by whether older (age ≥65 years) American patients have additional commercial or Medicaid insurance coverage. It is unknown whether mortality differs by type of insurance coverage for the approximate 1.5 million older Americans who annually survive a hospitalization necessitating intensive care.

Objective: To determine whether different types of insurance status are independently associated with a higher 1-year mortality rate among older survivors of critical illness.

Methods: We used the New York Statewide Planning and Research Cooperative System and American Hospital Association Annual Survey to conduct a retrospective cohort study of older (age ≥65 years) adults who had their first hospitalization with intensive care and who survived to discharge between January 1, 2010 and December 31, 2014 in New York State..

Measurements and Main Results: The primary outcome was mortality in the first year after hospital discharge. Of the 339,261 survivors of critical illness, 20% died within 1 year of hospital discharge. Compared to those with Medicare and commercial insurance, those with Medicare alone had no difference in 1-year mortality (adjusted hazard ratio [aHR], 1.01; 95% CI, 0.99-1.03), and those with Medicaid had a 7% higher 1-year mortality rate (aHR, 1.07; 95% CI, 1.05-1.09). Compared to whites, blacks had a similar 1-yr mortality rate, and Hispanic ethnicity was associated with better 1-year survival (aHR 0.87; 95% CI 0.84-0.89). The association between insurance status and mortality only varied among whites when the analysis was stratified by race. Whites with Medicaid had a 9% higher 1-year mortality rate when compared to those with Medicare and commercial insurance (aHR 1.09; 95% CI, 1.07-1.12). Analyses stratified on discharge location showed that the 1-year adjusted mortality rate did not vary by insurance status, Medicare alone and Medicaid, for those discharged home (aHR 0.99, 95% CI 0.96-1.02 and 0.99, 0.96-1.02), but was substantially greater for Medicaid recipients discharged to skilled-care facilities (aHR 1.18; 95% CI,1.15-1.21).

Conclusions: Mortality in the first year after critical illness is higher among older adults with Medicaid insurance compared to those with Medicare and additional commercial insurance, especially among those discharged to skilled-care facilities. Our findings should prompt future investigations into care disparities at skilled-care facilities that may mediate the higher mortality rates observed among these poor older survivors of critical illness .

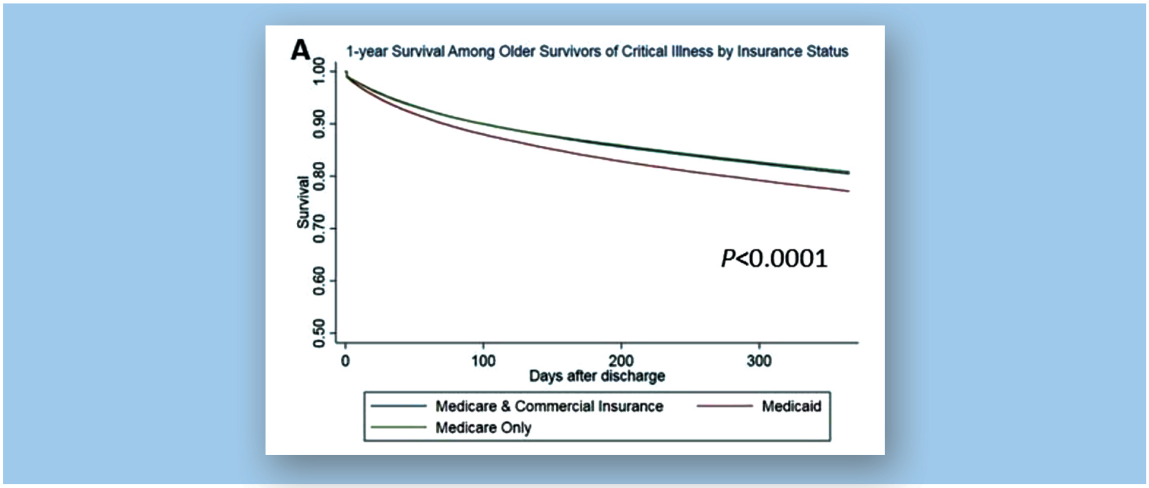

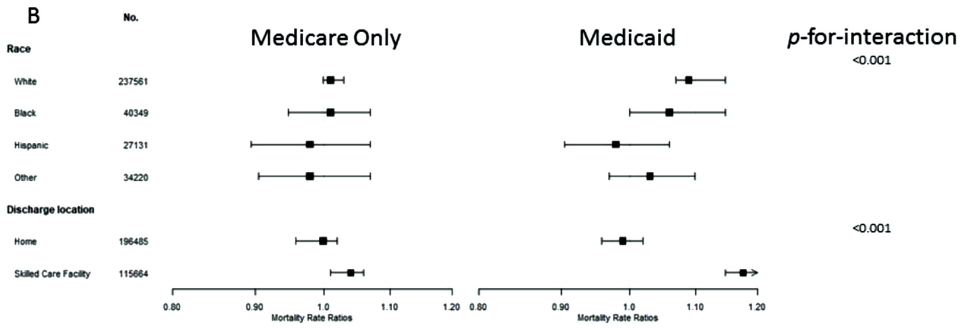

Figure1:(A) Kaplan-Meier survival curves by categories of insurance stats for older ICU survivors. (B) Stratified analyses across race and discharge location. Mortality rate ratios are compared to those with Medicare and commercial insurance.

Microbiome Communities in *Pseudomonas aeruginosa* Pneumonia

C.I. Pickens[1], P. Hountras[1], J. M.Walter[1], J.M. Kruser[1], C. Qi[1], B.D. Singer[1], S. Green[2], P. Seed[1,3], R.G. Wunderink[1]

[1]Northwestern University Feinberg School of Medicine, Chicago, IL, [2]University of Illinois Chicago, Chicago, IL, 3Ann and Robert H. Lurie Children's Hospital, Chicago, IL

Rationale: The discovery of a normal lung microbiome has forced re-examination of previous assumptions regarding the pathogenesis of pneumonia. Maintenance of a "normal" lung microbiome may prevent development of hospital-acquired pneumonia (HAP). *Pseudomonas aeruginosa* (PA) is one of the most difficult to treat etiologies of HAP. PA persistence is common despite appropriate antibiotics. Recurrent PA HAP is common, leading to suggestions that prolonged courses of treatment are necessary. We hypothesize that an altered lung microbiome cooperates with PA virulence to lead to poor clinical outcomes.

Methods: A convenience sample of 67 were collected from residual non-bronchoscopic and bronchoscopic BAL samples obtained for suspected pneumonia from patients intubated in any intensive care units. Cell count and differential, gram stain, and quantitative bacterial culture were performed on all BALs at time of collection. BAL nucleic acid extraction was performed, followed by library preparation and shotgun metagenomic sequencing (SMS). Taxonomic assignments of SMS reads were made using One Codex.. Unsupervised clustering via Weighted Gene Co-Expression Network Analysis (WGCNA) was used to define cooperative modules of microbial constituents associated with PA HAP.

Results: Results of WGCNA clustering are depicted as color-coded modules (A). Constituents of the Purple Module are listed in Panel B. A highly significant correlation between membership in the Purple Module and culture of a pathogen (Spearman correlation r- 0.81, p = 0.001) was found (Panel C). Presence of the Purple Module was significantly more likely in positive clinical PA cultures compared to negative cultures or all other pathogens with the possible exception of Acinetobacter (Panel D). Based on this unexpected association, BAL culture data from the last 5 years was reviewed: coinfection with PA occurred in 21 of 95 (22%) of positive Acinetobacter cultures. Coinfection occurred in 14% of positive PA cultures.

Conclusions: A specific microbiota cluster with PA in clinically documented pneumonia. This microbiome cluster may facilitate persistence or recurrence of PA pneumonia. Surprisingly, this microbiome cluster is also associated with *Acinetobacter* pneumonia, potentially explaining the not uncommon coinfection with these two pathogens.

Pulmonary Lymphatics Regulate Immune Cell Trafficking and Lung Injury

Hasina Outtz Reed, M.D. Ph.D. and Mark L. Kahn, M.D.

Department of Medicine, University of Pennsylvania, Philadelphia, PA

The pulmonary lymphatics are critical for lung function due to the unique susceptibility of the lung to inflammation and its relatively constant exposure to pathogens, immune cells, and inflammatory mediators. Previous studies have noted an association between increased or abnormal lymphatics in diverse lung diseases, but it is unclear whether lymphatics are protective or pathogenic in these settings. Unfortunately, investigating the role of pulmonary lymphatics in lung disease has been made difficult by a lack of functional models of impaired lymphatic function. We have generated two entirely novel models of impaired pulmonary lymphatic flow in mice, which for the first time allow for detailed investigation of the role of these vessels in lung function and whether they contribute to lung injury in pathogenic settings. Clec2-mutant mice have severely impaired lymph flow due to an absent platelet plug at the lympho-venous junction and retrograde flow of blood into the lymphatic system that prevents lymphatic drainage. We have also generated a second model of impaired lymphatic flow and induce diphtheria toxin-mediated cell death of lymphatic endothelial cells in mouse lung transplants. These mice have unilateral deletion of pulmonary lymphatics in the transplanted lung, with intact lymphatics in the native lung. We have found that impaired lymphatic flow leads to increased pulmonary inflammation and altered altered leukocyte trafficking, leading to the formation of tertiary lymphoid follicles within the lung parenchyma. Furthermore, formation of these lymphoid follicles was associated with significant lung parenchymal damage. Given the prevalence of tertiary lymphoid follicles in a variety of chronic lung disease, our studies raise the possibility that impaired lymphatic function may be a common mechanism in the pathogenesis of lung injury. Furthermore, our studies may change the current paradigm of the role of the pulmonary lymphatics and implicate that they are active players in lung biology..

Predicting Intensive Care Unit Readmission with Machine Learning using Electronic Health Record Data

Juan C. Rojas MD, Kyle A. Carey MPH, Dana P. Edelson MD, MS, Laura R. Venable MS, MPH, Michael D. Howell MD, MPH, Matthew M. Churpek, MD, MPH, PhD

Rationale: Patients transferred from the intensive care unit (ICU) to the wards who are later readmitted to the ICU have increased length of stay, healthcare expenditure, and mortality compared to those who are never readmitted. Improving risk-stratification for patients transferred to the wards could have important benefits for critically ill hospitalized patients. We aimed to use a machine-learning technique to derive and validate an ICU readmission prediction model with variables available in the electronic health record (EHR) in real-time and compare it to previously published algorithms.

Methods: We conducted an observational cohort study of all adult patients who received care at an academic hospital in an ICU and were subsequently transferred to the medical-surgical wards between November 1st, 2008 and January 15th, 2016. Patient characteristics, nursing assessments, ICD-9 codes from prior healthcare encounters, medications, ICU interventions, diagnostic tests, vital signs, and laboratory results were extracted from the EHR and used as predictor variables. For each predictor variable, the measured value closest to the time of ICU discharge was utilized. A gradient boosted machine learning model was fit in the training cohort, and accuracy for predicting ICU readmission was compared to the Stability and Workload Index for Transfer (SWIFT) score and Modified Early Warning Score (MEWS) in the validation cohort. All risk scores were calculated at the last ICU observation prior to ward transfer.

Results: A total of 24,885 ICU transfers to the wards were included, with 14,962 transfers (60%) in the training cohort and 9,923 transfers (40%) in the validation cohort. Eleven percent (2,834) of discharges to the wards were later readmitted to the ICU. The machine learning derived model had the highest AUC for predicting those patients ever readmitted (AUC 0.76 [95% CI 0.75–0.78]), followed by SWIFT (AUC 0.65 [95% CI 0.63–0.66]), and MEWS (AUC 0.58 [95% CI 0.56–0.60]); p value < 0.0001 for all comparisons. Blood urea nitrogen, Braden scale, oxygen saturation/FiO2 ratio, and albumin were the most important predictor variables in the machine learning model (Figure).

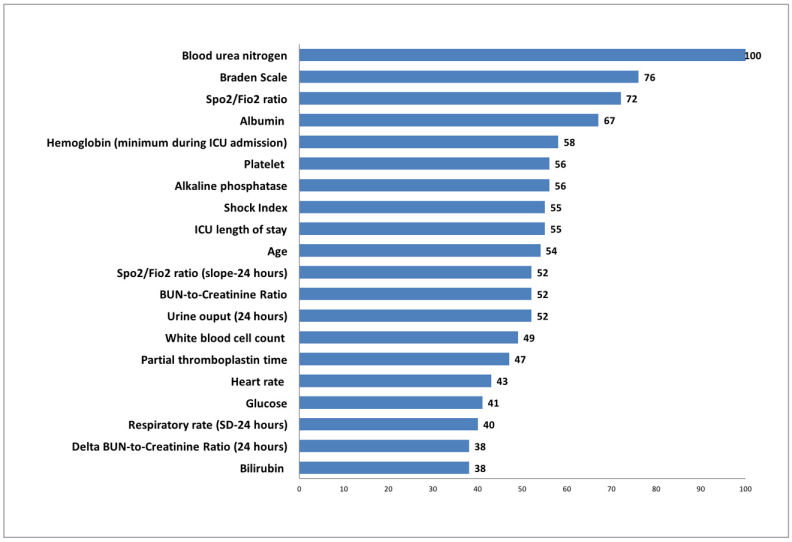

Figure. Twenty most important predictor variables in the gradient boosted machine model, scaled to a maximum of 100.

Conclusions: Our novel machine learning approach to predicting ICU readmission was significantly more accurate than previously published algorithms and used only data available in real-time. Implementation of this approach could target patients who may benefit from additional time in the ICU or more frequent monitoring after transfer to the hospital ward.

Inhaled corticosteroid (ICS) treatment is the cornerstone for achieving asthma control

Lesly Samedy, PharmD, PhD

University of California, San Francisco (UCSF)

Rationale: Glycogen synthase kinase-3β (GSK3β) is a highly conserved serine-threonine kinase that is a critical regulator of cell differentiation, metabolism, development, and inflammation. GSK3β-mediated phosphorylation is a key step in targeting substrates of Skp1/Cul1/F-box protein (SCF) E3 ubiquitin ligases to the proteasome for degradation. Recent data suggest that GSK3β has critical roles in propagating inflammation in murine models of acute lung injury. The goal of our study was to understand how GSK3β protein stability is regulated and how these mechanisms may influence inflammation in murine lung epithelial cells..

Methods: Site-directed mutagenesis was used to generate lysine to arginine point mutations in GSK3β. Plasmids expressing hemagglutinin (HA)-tagged wild-type, K183R, and K205R mutant GSK3β were transfected into murine lung epithelial cells (MLE-12). After cells were cultured for 48 h, a cycloheximide chase assay (40 μg/mL) was performed to evaluate the half-life of GSK3β. Lysates were collected at 0, 2, 4, and 8 h and immunoblotted for HA-tagged GSK3β. Plasmids were also transfected into MLE-12 cells and after 48 h of culture, cells were treated with proteasome inhibitor MG132 (20 μM) to allow accumulation of polyubiquitinated proteins. Lysates were immunoprecipitated for HA-GSK3β and immunoblotted with antibody for K48-linked ubiquitin. Lysates from a HEK293 expression library of over 30 F-box proteins were immunoblotted for endogenous GSK3β. Plasmid expressing histidine (V5)-tagged FBXO17 was also transfected into MLE-12 cells. Lysates were prepared after 48 h and immunoblotted for GSK3β.

Results: We identified lysine 183 as the primary acceptor site for K48-linked ubiquitin chains in GSK3β. K183R mutant GSK3β protein had a longer half-life and significant reduction in polyubiquitination than wild-type or K205R-GSK3β. Finally, we identified FBXO17 as a subunit of an SCF E3 ubiquitin ligase complex that targets GSK3β for polyubiquitination and proteasomal degradation in lung epithelial cells.

Conclusions: Our study characterizes a previously unknown mechanism for GSK3β degradation by the proteasome. We have identified FBXO17 as a subunit of an SCF E3 ligase complex that targets GSK3β. Future studies will focus on characterizing how FBXO17 modulates inflammation in lung epithelial cells. Our data suggest a critical role for the ubiquitin-proteasome pathway in regulating active and inactive pools of GSK3β which may influence the severity of lung inflammation.

REDUCED CAVEOLIN 1 COMPROMISES CYSTIC FIBROSIS BRONCHIAL EPITHELIAL CELL BARRIER FUNCTION

Sendon CS[1], Oez H1, Zhang PX[1], Barone C[1], Di Pietro C[1], Pierce R[1], Egan ME[1,2], Bruscia EM[1]

[1]Department of Pediatrics Pediatric Pulmonary Department and [2]Cellular Molecular Physiology, Yale University School of Medicine, New Haven CT, USA

Objectives: The bronchial epithelium has a critical role as a mechanical cell barrier that, when impaired, leads to an excessive inflammation and poor defense against microorganisms. The cell barrier permeability is regulated by cell junction proteins, which have been recently found to be compromised in Cystic Fibrosis (CF)-affected human bronchial epithelial cells (HBECs). Caveolin-1 (CAV1), a scaffolding membrane protein, is an important regulator of cell barrier function. We aim to investigate whether CAV1 levels are reduced in CF-affected HBECs, and if this reduction alters CF HBEC barrier function in response to inflammatory stimuli.

Methods: We used: a) mouse lung tissues (MLT); b) tracheal epithelial cells (mTECs) grown at air-liquid interface from CF and WT mice; c) CFBE41o- (CF) and 16HBE14o– (non-CF) HBEC lines; d) CFBE41o- overexpressing WT of F508del CFTR; and e) newly developed 16HBE14o– in which CFTR was stably knocked-down using lentiviral vectors (LV) expressing shRNA against CFTR. Two shRNAs against CFTR, CF1 and CF2 or scramble shRNA as control were tested. CFTR knockdown in 16HBE14o–was validated by qPCR and CFTR function, as assessed by Ussing chamber assay. CAV1 expression was assessed at baseline and after LPS challenge in the various cells/tissue via qPCR or western blot. Electric Cell-substrate Impedance Sensing (ECIS®) was used to measure cell barrier permeability in response to LPS. Impedance was measured before and after LPS exposure and changed in impedance to LPS (Z_{LPS}- $Z_{baseline}$) was assessed.

Results: MLT from CF mice (F508del/F508del) have decreased CAV1 levels compared to WT controls. CAV1 expression was reduced in CF-KO mTECs, CFBE41o- (CF), as well as, in CFBE41o- cells overexpressing F508del CFTR compared to matched WT controls. This was observed before and after LPS challenge (*$p<0.05$). To directly study the effect of CFTR on CAV1 expression and barrier function, we developed 16HBE14o– cells in which CFTR was knocked-down via shRNA. qRT-PCR showed that shRNA-CF1 and shRNA-CF2 efficiently downregulate expression of CFTR in 16HBE14o–. 16HBE/shRNA-CF1 cells shown minimal CFTR function. In contrast, 16HBE/shRNA-CF2 retained some CFTR function. 16HBE/shRNA-CF1 had lower CAV1 levels compared to 16HBE/shRNA-CTR. Consistently, the change in impedance in response to LPS was lower in 16HBE/shRNA-CF1 compared to 16HBE/shRNA-CTR.

Conclusions: CAV1 expression is reduced in murine CF lungs, CF mTEC and CF HBEC lines. Moreover, knocking-down CFTR in 16HBE14o– cells recapitulated the reduced expression of CAV1 and altered impedance change in response to LPS, suggesting that loss of CFTR function increases cell barrier permeability in response to LPS.

FBXO17 Activates Akt and Increases Survival of Lung Epithelial Cells

T. Suber, I. Nikolli, J. Zhao, R. Mallampalli, Y. Zhao

University of Pittsburgh School of Medicine - Pittsburgh, PA/US

Rationale: The Skp1/Cul1/F-box (SCF) family of E3 ubiquitin ligases targets many substrates that mediate acute lung injury and inflammation. Prior work from our group identified FBXO17 as a novel F-box protein that targets glycogen synthase kinase-3β (GSK3β) to the proteasome and downregulates inflammatory responses in lung epithelial cells. Given the role of GSK3β in opposing Akt/PKB (protein kinase B) activity in the mammalian target of rapamycin complex 1 (mTORC1) pathway, we examined whether increased FBXO17 expression enhanced Akt activity and cell survival.

Methods: FBXO17 was cloned into pcDNA 3.1 vector containing hemagglutinin (HA) or histidine (V5) tags. Plasmids expressing FBXO17 or empty vector were transfected into human A549 lung epithelial cells using Lipofectamine 2000. After 48 h, lysates were prepared and analyzed by immunoblotting for Akt, p-Akt, survivin, and β-actin (loading control) protein expression. Knockdown experiments were conducted using scrambled and *siFBXO17* small interfering RNA (Integrated DNA Technologies). RNA was isolated from A549 cells and quantitative real-time PCR was performed using primers for *AKT1* and *ACTB* (control). Cell viability was analyzed after transfection using a colorimetric, tetrazolium-based assay (Promega).

Results: BXO17 overexpression induces robust Akt and mTOR phosphorylation without influencing mRNA transcript levels. Silencing FBXO17 gene expression reduces Akt phosphorylation. Ectopic FBXO17 expression was associated with significantly increased epithelial cell viability and metabolic activity.

Conclusions: Through negative regulation of GSK3β by FBXO17-mediated proteasomal degradation, Akt activity increases and thus leads to increased cell survival. This data suggests that FBXO17 may be implicated in remodeling and repair of lung epithelium after injury given the critical role of the PI3K/Akt/mTOR pathway in these mechanisms. Future mechanistic and translational studies will evaluate how FBXO17 may modulate the mTORC pathway in experimental models of acute lung injury.

Funding sources: Merit Review Award from the US Department of Veterans Affairs and National Institutes of Health, R01 grants HL096376, HL097376, HL098174, HL081784, 1UH2HL123502, and P01 HL114453 (to R.K.M.), NIH R01 HL131665 (to Y.Z.), F32 HL137248 and the Burroughs Wellcome Fund (to T.L.S.).

Expression of the Tumor Suppressor WWOX in Pulmonary Artery Smooth Muscle Cells Is Lost During Hypoxia

M. Gomes[1], S. Singla[2], J. Chen[2], R. F. Machado[1]

[1]Division of Pulmonary, Critical Care, Sleep, and Occupational Medicine, Indiana University, Indianapolis, IN, United States, [2]Division of Pulmonary, Critical Care, Sleep, and Allergy, University of Illinois at Chicago, Chicago, IL, United States.

Introduction: The human WWOX gene, encompassing the chromosomal fragile site FRA16D, encodes a tumor suppressor. WWOX is a WW domaincontaining oxidoreductase that enhances efficient DNA damage response (DDR) functions ranging from DNA repair and apoptosis to suppression of tumorigenic signaling pathways. Loss of WWOX expression due to gene deletions, loss of heterozygosity, chromosomal translocations, or epigenetic silencing is frequently observed in human malignant cancer cells, which is associated with a worse prognosis. Pulmonary Arterial Hypertension (PAH) is characterized by pulmonary artery smooth muscle cell (PASMC) apoptosis-resistant hyperproliferation which contributes to obliterative pulmonary vascular remodeling. According to these observations, we hypothesize that reduction in WWOX expression may promote vascular remodeling in PAH.

Methods and Results: When compared to normoxia, PASMCs isolated from PAH patients showed decreased mRNA and protein WWOX levels after 6 and 24 hours of hypoxia (3% O2) exposure ($P<0.0001$ for mRNA; $P=0.0134$ for protein, respectively). Furthermore, lungs obtained from rat models of pulmonary hypertension (Sugen plus hypoxia mediated PH and monocrotaline-induced PH) showed protein levels of WWOX reduced by 40% and 60% respectively, when compared to control lungs ($P<0.05$). A similar pattern was found when mice were exposed to 4-weeks of 10% hypoxia, WWOX expression in lung tissue was significantly reduced, especially after 28 days, where WWOX expression in hypoxia was 80% lower than in normoxia ($P=0.01$). hPASMCs incubated under hypoxia (3% O2) showed a time-dependent decrease in WWOX mRNA ($P<0.05$) and protein expression ($P=0.0076$). In addition, WWOX overexpression in hPASMCs resulted in upregulation of Bax, and elevated levels of cleaved caspase-3, indicating activation of the intrinsic apoptosis pathway. Conversely, WWOX-silencing siRNA increased hPASMC proliferation by 60% ($P=0.001$) in a BrDU cell proliferation assay. Suppression of WWOX expression appears to modulate cell cycle progression with a downregulation of both p21 cyclin-dependent kinase inhibitor (p21 Waf1/Cip1) and Cyclin B expression.

Conclusions: WWOX expression is decreased during hypoxia in vivo and in vitro. Attenuation of WWOX expression increases cell proliferation while WWOX overexpression promotes apoptosis, suggesting that these events can contribute to the pathobiology of PAH and overexpression of WWOX may be a therapeutic strategy for PAH. Further studies are ongoing to better understand the mechanisms associated with these effects..

Tuberous Sclerosis and Lymphangioleiomyomatosis are Neurocristopathies

Uchenna J Unachukwu[1], Takayuki Shiomi[1, 2], Jarrod Sonett[1], Denzel Woode[1], Vincent Anguiano[1, 3], Monica P. Goldklang[1], Christopher Damoci[4], Kiran Chada[5], Jeanine D'Armiento[1]

[1]Center for LAM and Rare Lung Disease, Department of Anesthesiology, College of Physicians and Surgeons, Columbia University, 630 West 168th Street, New York, NY 10032, USA. [2]Department of Pathology, International University of Health and Welfare, School of Medicine, 4-3 Kouzunomori, Narita-shi, Chiba 286-8686, Japan. [3]Graduate School of Biomedical Sciences, Icahn School of Medicine at Mount Sinai. 1 Gustave L. Levy Pl, New York, NY 10029. [4]Small Animal Imaging Shared Resource, The Herbert Irvin Comprehensive Cancer Center, Columbia University Medical Center, 1130 St. Nicholas Avenue, New York, NY 10032, USA. [5]Department of Biochemistry, Rutgers-Robert Wood Johnson Medical School, Rutgers University, 675 Hoes Lane, Piscataway, NJ 08854, USA.

Introdution and Rationale: Tuberous Sclerosis (TS) and its pulmonary manifestation, lymphangioleiomyomatosis (LAM), are rare disorders characterized by widespread harmatomas and benign neoplasms in multiple organs. These disorders are linked to loss-of-function mutations in Tsc1 or more often Tsc2 tumor suppressor genes, triggering dysregulation of the mechanistic target of rapamycin (mTOR) pathway. Given the variably limited success obtained using mTOR pathway inhibitors for TS and LAM therapy, understanding the source of heterogeneous cells comprising TS and LAM tumors and their method of propagation throughout the body will infom more effective treatment strategies. As LAM presents in multiple organs and expresses markers of early progenitor cells including High Mobility Group A2 (HMGA2), we postulated that LAM and TS are neurocristopathies.

Methods: A $Tsc2^{+/-}Mpz(Cre)^{fl/fl}$ TS reporter mouse model expressing cre recombinase specifically in neural crest and schwann cells under the control of myelin protein zero (MPZ) promoter was generated and aged for 1.5 years along with age-matched control ($Tsc2^{+/+}Mpz(Cre)^{fl/fl}$, $Tsc2^{+/+}Mpz(Cre)^{+/+}$) mice to allow for tumor development. IVIS spectral imaging, and small animal ultrasound and magnetic resonance imaging (MRI) were used to detect the occurrence of tumors. Tumors were excised and immunohistochemical sections prepared and stained for the expression of neural crest markers. Neural crest marker expression in $Tsc2^{+/-}$ mouse tumors was confirmed using RT-PCR and Western blots.

Results: Tumors were detected only in $Tsc2^{+/-}Mpz(Cre)^{fl/fl}$ mice compared to age-matched control mouse groups. Additionally, only immunohistochemical slices obtained from renal and hepatic tumors of this TS reporter mouse model exhibited td-Tomato expressing tumor cell masses specifically annotating neural crest ontogeny in tumors of this mouse group. Upon staining for neural crest markers, tumorigenesis in the TS reporter mouse model was observed to be propagated by cranial neural crest cell (CNCC) subpopulations selectively expressing delaminating late-migratory neural crest marker β-1, 3-glucoronyltransferase 1 (CD57) and melanoma-initiating nerve growth factor receptor (NGFR/p75 NTR) but not transcription factor activating protein (Tfap2α). This differential marker expression was observed only in tissue slices obtained from renal tumors and not hepatic tumors indicating tissue specificity in neural crest-derived tumor occurrence initiated by *Tsc2* haploinsufficiency. Results were confirmed using RT-PCR and Western blots.

Conclusions: We propose that pathogenic cells in TS and LAM delaminate and migrate from the neural crest during neurocristogenesis forming cranial neural crest sub-populations that give rise to craniofacial mesenchyme and peripheral nervous tissues. Domiciled in these organs, these cells co-opt tumorigenesis upon secondary somatic *Tsc2* mutations and/or environmental stimuli.

Airway Surface Liquid Antimicrobial Activity Follows a Seasonal Pattern

L. G. Vargas Buonfiglio[1], O. G. Vanegas Calderon[2], A. K. Gerke[1], P. Polgreen[1], J. Zabner[1], A. P. Comellas[1]

[1]Internal Medicine, University of Iowa, Iowa City, IA, United States, [2]Pediatrics, University of Iowa, Iowa City, IA, United States.

Rationale: Airway infections follow a seasonal pattern characterized by increased infections during winter compared to summer. One proposed mechanism is that during winter there is more prevalence of vitamin D3 deficiency due to a decrease in total sun exposure. The airway surface liquid (ASL) antimicrobial activity is part of the innate immune mechanism that prevents airway infections. Many antimicrobial peptides in the ASL are upregulated by vitamin D3. We hypothesized that the ASL antimicrobial activity will be greater during the summer compared to the winter months.

Methods: 40 voluntaries from Iowa underwent bronchoscopies with ASL collection between January and December of 2008-2009. We performed an analysis of the antimicrobial activity of human ASL collected via bronchoscopy against ~5x105 CFU of a bioluminescent S. aureus. We interpreted a reduction in Relative Light Units (RLU) at 4 minutes as ASL antimicrobial activity. We grouped the subjects by months when the ASL was collected and plotted the average of RLU along with the total hours of sunshine for the state of Iowa. Serum concentration of active vitamin D3 (1,25(OH)2D3) were also measured.

Results: We found that the ASL antimicrobial activity gradually changed following a seasonal pattern. In addition, we found that both ASL antimicrobial activity and levels of 1,25(OH)2D3 were significantly higher in the summer (June –August) compared to the winter time (December-February). This is the first report that suggests that the airway may have an intrinsic seasonal antimicrobial activity. We proposed that levels of vitamin D3 may play a role in this effect. Additional studies must determine other alternative mechanisms responsible for this phenomenon.

Effect of Opioid Abuse and Dependence on Outcomes of Patients Hospitalized with Pneumonia: a 5 Year Analysis

Fernando Vazquez de Lara[1,2], Di Pan[1,2], Felipe Bolivar[1,2], Valeria Santibanez[1,2], Joseph Mathew[1,3]

[1]Mount Sinai St. Lukes and Mount Sinai West Hospitals, New York, NY, United States, [2]Division of Pulmonary and Critical Care Medicine, Mount Sinai St. Lukes and Mount Sinai West Hospitals, New York, NY, United States, [3]Department of Medicine, Icahn School of Medicine at Mount Sinai, New York, NY, United States

Rationale: Prior studies have shown that opioid use can increase the risk of pneumonia and have a negative impact on the immune system. The aim of this study is to analyze the outcomes of patients admitted for pneumonia with a history of opioid abuse or dependence.

Methods: This is a retrospective propensity score matched analysis utilizing the 2010 to 2014 Nationwide Inpatient Sample, the largest inpatient database in the United States. The study population comprised of 29,455 patients over age 18 with a primary diagnosis of pneumonia with and without a secondary diagnosis of opioid abuse or dependence. The outcomes of interest were mortality, non-invasive ventilation (NIV) use, endotracheal intubation and length of stay. Multivariate logistic regression was performed to test for independent associations between variables of interest. Diagnoses and procedures were identified using ICD-9-CM codes. Analysis was performed using STATA 14.2.

Results: Patients in the opioid group were more likely to be intubated during hospitalization when compared to non-opioid users (OR 1.45, p<0.05). However, mortality was reduced in the opioid group (OR 0.53, p<0.05). NIV utilization did not differ among the groups (OR 1.05 p=0.754) and no difference in length of stay was found (-0.042 days, p=0.82).

Conclusions: Opioid dependence and abuse increase the risk of intubation but seem to decrease mortality in hospitalized patients admitted for pneumonia. No differences were seen in NIV utilization or length of stay. Further research is needed to better understand the role of chronic opioid use and abuse in patients admitted for pneumonia.

Patient characteristics	No opioid use/abuse		Opioid use/abuse			
	No.	%	No.	%	p value	
No. (%) of patients	14644.44	49.7	14811.96	50.3		
Women, no. (%)	7121.851	48.6	7211.57	48.7		
Race/ethnicity no. (%)						
White	19217	0.6524	18884	0.6411	0.6133	
Black	6816	0.2314	6542	0.2221	0.6558	
Hispanic	2860	0.0971	3025	0.1027	0.1804	
Asian or Pacific Islander	100	0.0034	159	0.0054	0.6016	
Native American	80	0.0027	147	0.005	0.1809	
Other	383	0.013	698	0.0237	0.0134	
Mean age, years	51.14		51.24		0.8406	
Charlson comorbidity Index score, no (%)						
>3	8289	0.2814	8083	0.2744	0.5626	
4-5	9800	0.3327	9765	0.3315	0.9300	
6-7	4463	0.1515	4507	0.153	0.8712	
>8	6904	0.2344	7099	0.241	0.6487	
Insurance type						
Medicare	10209	0.3466	10260	0.3483	0.9204	
Medicaid	10975	0.3726	11114	0.3773	0.7672	
Private	4468	0.1517	4315	0.1465	0.6451	
Uninsured	3806	0.1292	3767	0.1279	0.9185	
Hospital characteristics						
Hospital bed size						
Small	4015	0.1363	4245	0.1441	0.6212	
Medium	8424	0.286	8386	0.2847	0.9593	
Large	17017	0.5777	16828	0.5713	0.8247	
Hospital region						
Northeast	11517	0.391	10195	0.3461	0.1304	
Midwest	4259	0.1446	4421	0.1501	0.6808	
South	7087	0.2406	9011	0.3059	0.0130	
West	6592	0.2238	5829	0.1979	0.3429	
Teaching hospital, no. (%)	13397	0.4548	15544	0.5277	0.0142	
Results	**No opioid use/abuse**		**Opioid use/abuse**		**Odds Ratio (95% CI)**	**p value**
	No.	%	No.	%		
Mortality	205	1.40	110	0.74	**0.53 (0.30-0.94)**	**0.031**
Intubated	394	2.69	574	3.88	**1.45 (1.03-2.04)**	**0.031**
NIV	586	4.00	597	4.03	1.05 (0.79-1.38)	0.754
Length of stay (mean days)	5.103487		5.147088		-0.04 (-.042-0.33)	0.825

A recurrent hemizygous deletion at the MHC region impacting MICA, LINC01149, HCP5, HCG26 associates with idiopathic pulmonary hemosiderosis (IPH)

Gerardo Vazquez Garcia, Xiao Chang, Frank Mentch, Athena Zuppa, Samuel Goldfarb, Hakon Hakonarson

Idiopathic pulmonary hemosiderosis (IPH) is a rare disease that occurs mainly in childhood. This disease is characterized by recurrent episodes of diffuse alveolar hemorrhage (DAH). This could be cause by different conditions such as infections, pulmonary hypertension or rheumatologic disease. IPH is only diagnosed, when there is no underlying cause of DAH. Several pathophisiologic pathways have been suggested. Prior pathology studies have described, diffuse fibrosis, hemosiderosis, and degeneration of elastic fibers. This suggests that structural defects in the alveolar capillaries basement membrane may be a predisposing factor of IPH. The response to immunosuppressive therapies suggests and immune mediated process. Additionally, there has been several reports of familial clustering, suggesting a possible genetic predisposition to this disease. The purpose of this study was to determine if there is a genetic influence on the phenotype of IPH and the response to treatment.

We recruited 10 patients with IPH and genotyped them using an Illumina SNP array. Genome-wide association study was conducted on all 10 cases, including 7 African-American children with IPH and 200 ancestry-matched healthy controls, as well as 3 European-American children with IPH and 200 healthy controls.

As expected, the GWAS analysis did not identify a SNP having a P-value less than 10e-5 in either population. We further performed a meta analysis to combine the association results from two studies, and identified two SNPs with a P-value less than 10e-5 (rs7530150, 2.14e10-6 ; rs17064334, 4.16e10-6). rs7530150 is located 1p31.3 within the gene PDE4B. rs17064334 is located at 4q34.3 near gene NEIL3. We performed a genome-wide copy number variation analysis on the same cohort and found a recurrent ~90Kb hemizygous deletion at the MHC region (chr6: 31360389-31451476; Gene: MICA, LINC01149, HCP5, HCG26). The CNV was found in one Caucasian and one African-American case, and in two Caucasian and two African-American controls. Fisher's exact test suggests this deletion may confer risk to IPH (P-value = 0.0076).

We have conducted both GWAS and CNV analysis on a small cohort of thoroughly phenotyped IPH patients. Although the sample size is small, this is the first effort to explore potential genes underlying IPH. We found a ~90Kb hemizygous deletion located at the MHC region that is significantly associated with IPH suggesting IPH may be associated with HLA genes at the MHC locus. Future direction includes; recruitment of 30 subjects for genotype and analysis, characterization of the cohort response to steroids and the relationship with this deletion.

.

Diagnosis and Management of COPD in HIV-infected Individuals: Opportunities for Improvement

J. S. Zifodya[1], M. Triplette[2], S. Shahrir3, E. Attia4, K. M. Akgun[5], G. W. Soo Hoo[6], C. Wongtrakool[7], M. C. Rodriguez-Barradas[8], J. P. Tate[9], K. A. Crothers[10]

[1]Pulmonary and Critical Care, University of Washington, Seattle, WA, United States, [2]Medicine, University of Washington and Clinical Research Division, Fred Hutchinson Cancer Research Center, Seattle, WA, United States, [3]University of Washington, Seattle, WA, United States, [4]Pulmonary/Critical Care Medicine, University of Washington, Seattle, WA, United States, [5]Internal Medicine, VA Connecticut Healthcare System and Yale University, Madison, CT, United States, [6]Pulmonary and Critical Care, VA Medical Ctr W Los Angeles, Los Angeles, CA, United States, [7]Medicine, Atlanta Veterans Affairs Medical Center, Atlanta, GA, United States, [8]Infectious Disease, Michael E. DeBakey Veterans Affairs Medical Center and Department of Medicine, Baylor College of Medicine, Houston, TX, United States, [9]Veterans Affairs, Connecticut Healthcare System and Yale University School of Medicine and Public Health, West Haven, CT, United States, [10]Division of Pulmonary and Critical Care, University of Washington, Seattle, WA, United States.

Rationale: Previous studies suggest a high rate of both misdiagnosis and inappropriate treatment for chronic obstructive pulmonary disease (COPD) in the general population, but have not included HIV-infected (HIV+) individuals. In this study, we examined the appropriateness of diagnosis and treatment of COPD in HIV+ and uninfected (HIV-) patient.

Methods: This is a secondary analysis of the Examinations of HIV Associated Lung Emphysema (EXHALE) study, which enrolled smoking-matched HIV+ and HIV- Veterans at four Veterans Affairs (VA) Medical Centers participating in the Veterans Aging Cohort Study (VACS) between 2009-2012. Clinical diagnosis of COPD was defined by International Classification of Diseases 9 (ICD-9) related diagnosis codes prior to baseline enrollment. Spirometrically-defined COPD was determined from enrollment post-bronchodilator spirometry ratio of forced expiratory volume in 1 second (FEV1) to forced vital capacity (FVC) < 0.7. Medication prescriptions were collected from VA electronic health records. We compared ICD-9 diagnosis of COPD to spirometry-based diagnosis, and examined medication prescriptions in the year before and after enrollment. We compared HIV+ and HIV- participants using Chi-squared testing.

Results: A total of 170 HIV+ and 145 HIV- participants were included in this study. Prior ICD-9 COPD diagnosis was identified in 46, and 64 had spirometry-defined COPD. 60% of participants with an ICD-9 COPD diagnosis did not have spirometry-defined COPD, and 73% with spirometry-defined COPD lacked prior ICD-9 COPD diagnosis. Proportions were similar by HIV status. Among participants with an ICD-9 COPD diagnosis, only 28% were prescribed any long-acting controller medications in the year prior to study enrollment. Inhaled corticosteroids (ICS) were the most common long-acting medication prescribed to both HIV+ and HIV- patients (Table). Long-acting beta-agonists (LABAs) or muscarinic antagonists (LAMAs) were less commonly prescribed, particularly among HIV+ participants (p=0.06 for LABA). 16 participants had ICD-9 diagnoses of both COPD and asthma, of which only 5 were on ICS. Prescription of long-acting inhalers did not appear to increase in the year after enrollment in those with spirometry-diagnosed COPD.

Conclusions: COPD was frequently both misdiagnosed and undiagnosed in HIV+ and similar HIV- participants. Most participants with ICD-9 or spirometry-defined COPD were not prescribed long-acting inhalers, and among those that were, ICS were the most common medication. Inappropriate ICS use may be of particular concern in HIV+ individuals given the increased risk of pneumonia and medication interactions. Implementation strategies to improve guideline-concordant COPD diagnosis and management are needed as HIV+ patients are aging with increasing prevalence of comorbid COPD.

Table. Percentage of patients with ICD-9 COPD diagnosis who have long-acting controller medications by HIV status

Prescription by inhaler type	HIV+ with ICD-9 COPD diagnosis		HIV- with ICD-9 COPD diagnosis	
	1 yr prior PFT	1 yr post PFT	1 yr prior PFT	1 yr post PFT
ICS	21%	29%	23%	27%
LABA	4%	17%	23%	18%
LAMA	8%	4%	5%	14%

HIV+ : HIV-infected;
HIV- : HIV-uninfected;
COPD: chronic obstructive pulmonary disease;
ICS: inhaled corticosteroids;
LABA: long acting beta-agonists;
LAMA: long acting muscarinic antagonists

American Thoracic Society International Conference

ATS 2019

See you in Dallas!

May 17-May 22, 2019

conference.thoracic.org

ATS 2019

Where today's science meets tomorrow's care™

NOTES

25 Broadway, 18th Floor, New York, NY 10004
t. 212-315-8600 | thoracic.org